Inorganic Chemistry

Article

pubs.acs.org/IC

Is Single-4-Ring the Most Basic but Elusive Secondary Building Unit That Transforms to Larger Structures in Zinc Phosphate Chemistry?

Aijaz A. Dar, Sunil K. Sharma, and Ramaswamy Murugavel*

Department of Chemistry, Indian Institute of Technology—Bombay, Powai, Mumbai 400076, India

Supporting Information

ABSTRACT: Haloaryl phosphates (X-dippH$_2$, X = Cl, Br, I) react with zinc acetate in the presence of collidine or 2-aminopyridine (2-apy) to yield zinc phosphate clusters [Zn(X-dipp)(collidine)]$_4$ (X = Cl (**1**), Br (**2**), I (**3**)) and [Zn(X-dipp)(2-apy)]$_4$·2MeOH (X = Cl (**4**), Br (**5**), I (**6**)), respectively. Single-crystal X-ray diffraction studies reveal that collidine and 2-apy capped zinc phosphates **1**−**6** exist as discrete tetrameric zinc phosphate molecules, exhibiting a cubane-shaped D4R core. In contrast, when the same reaction has been carried out in the presence of 4-cyanopyridine (4-CNpy), polymeric zinc phosphates {[Zn$_4$(X-dipp)$_4$-(4-CNpy)$_2$(MeOH)$_2$]·2H$_2$O}$_n$ (X = Cl (**7**), Br (**8**), I (**9**)) have been isolated. Compounds **7**−**9** are square-wave-shaped, one-dimensional polymers composed of fused S4R repeating units. The common structural motif found both in D4R cubanes **1**−**6** and polymers **7**−**9** is the S4R building block, which presumably undergoes further fusion because of the coordinative unsaturation at zinc and the simultaneous presence of free P═O. The closed shell cubanes **1**−**6** are obviously formed by a *face-to-face* dimerization involving two S4R units in which the two P═O groups are in cis-configuration. On the other hand, the one-dimensional (1-D) square-wave polymers **7**−**9** are formed from a face-to-face association of S4R building units in which the two P═O groups are in a trans-configuration. In order to stabilize these elusive S4R zinc phosphates, the reaction between Cl-dippH$_2$ and zinc acetate was carried out in the presence of excess imidazole as an ancillary ligand (1:1:4), although only an imidazole decorated cubane cluster [Zn(Cl-dipp)(imz)]$_4$.2MeOH (**10**) was isolated. The chelating *N*,*N*′-donor 1,10-phenanthroline ligand was used to eventually isolate cyclic S4R phosphate [Zn(μ_2-Cl-dipp)(1,10-phen)(OH$_2$)]$_2$·MeOH·H$_2$O (**11**). The change of Zn^{2+} source to zinc nitrate and the phosphate source to 2,6-dimethylphenyl phosphate (dmppH$_2$) led to the isolation of another polymeric phosphate [Zn(dmpp)(MeOH)]$_n$ (**12**), with a zigzag backbone, formed through an *edge-to-edge* to polymerization of S4R building units with P═O groups in trans-configuration. The isolation of four different structural types of zinc phosphates **A**−**D** in the present study can be rationalized in terms of fusion of S4R rings in a variety of ways to either produce discrete clusters or 1-D polymers.

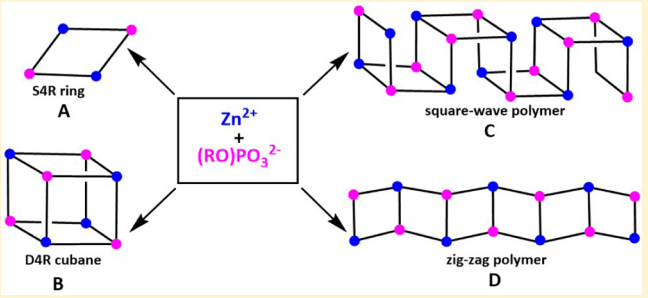

1. INTRODUCTION

Investigations on the chemistry and applications of porous/framework metal phosphate materials have progressed in great strides since the first isolation of aluminophosphates (AlPOs) by Flanigen and co-workers in the 1980s.[1] Over the years, these phosphate porous materials have found applications in diverse fields ranging from industry to agriculture to pharmacy.[2−6] During the initial stages of development, metal phosphate chemistry was mainly dominated by the isolation of polymeric species of various dimensionalities.[7−9] The recent realization, that these larger solids can be built from molecular precursors, has fueled the research activity in the field of molecular metal phosphates.[10] The knowledge of mechanism of transformations or Aufbau principle pertaining to these complex molecules is very limited. Part of this problem can be alluded to the fact that these materials are often synthesized by hydrothermal synthetic methods, which do not offer sufficient scope for control over reactivities.[11] However, structural investigations of these complex three-dimensional (3-D) structures with diverse architectures reveal that the basic building units involved in the formation of these materials are actually few in number. For example, in aqueous phase chemistry of aluminophosphates, S4R secondary building units have been observed as prominent SBUs among higher metallophosphates, which are presumed to be formed by a dissolution−reprecipitation mechanism or topochemical transformations aided by suitable rotation and condensation.[12] Transformations involving these building blocks are often empirical without much control on the reaction kinetics and products. Being the simplest units in these framework compounds, the association behavior and reactivity of S4R units must be investigated in detail, since it is believed that D4R, D6R, D8R, and other higher-member SBUs are formed from these four-membered ring units.[13] There are very few examples of independent molecular S4R units in the literature, which notably include studies on isolation, *in situ*

Received: March 2, 2015
Published: May 4, 2015

DOI: 10.1021/acs.inorgchem.5b00495
Inorg. Chem. 2015, 54, 4882−4894

solution characterization, and further extension of anionic S4R zinc phosphates into higher solids.[4a,b,7b] The expansion of these rings into porous metallophosphates is still largely an unsolved puzzle.[7b,14]

It has been recently established that the reaction of zinc acetate with the phosphate monoester (2,6-disopropylphenyl phosphate, dippH$_2$), in the presence of ancillary ligands (L) instantaneously results in the isolation of double-4-ring (D4R) zinc phosphates, [Zn(dipp)(L)]$_4$. These tetrameric phosphates, in turn, can be employed as secondary building units (SBUs) to build zinc phosphate framework solids via replacement of terminal ancillary ligands by a ditopic spacer, such as 4,4′-bipyridine.[6] Alternatively, even simple secondary interactions such as intercubane hydrogen bonds emanating from amino or hydroxyl functional groups appropriately placed on the ancillary pyridyl ligands have also been employed to assemble full hydrogen-bonded framework solids.[15]

Studies so far carried out on dippH$_2$-derived zinc phosphates have clearly shown that the D4R cubane formation is the most facile form of association. It has been envisaged in the present study that the functionalization at the 4-position of the aryl ring of the phosphate ligands can open up the possibility of covalently linking the cubanes at the phosphate end rather than at the zinc end. Toward this objective, we have recently investigated a series of *p*-haloaryl phosphates, which can be functionalized across the C−X bond to produce new C−C linked aryl phosphates.[16] These *p*-haloaryl phosphates have been employed in the present study as advantageous precursors for the synthesis of structurally diverse forms of zinc phosphates. The details of our findings are presented in this contribution.

2. RESULTS

2.1. Syntheses and Structures of Halogen Functionalized Discrete D4R-Zn-Cubanes 1−3. A 1:1:1 stoichiometric reaction of [Zn(OAc)$_2$·2H$_2$O] with X-dippH$_2$ in the presence of 2,4,6-trimethylpyridine (collidine) in methanol at room temperature produces zinc phosphates [Zn(X-dipp)(collidine)]$_4$ (X = Cl (**1**), Br (**2**), I (**3**)) (Scheme 1). The

Scheme 1. Synthesis of Compounds 1−6

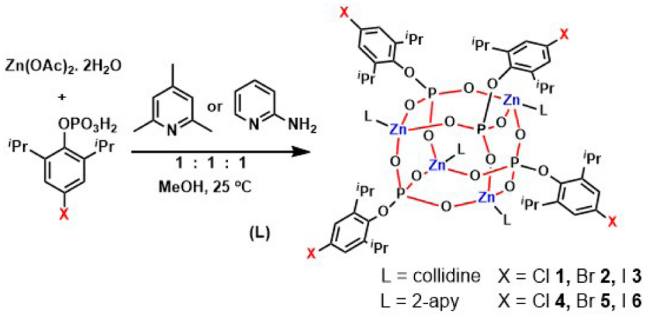

crystalline products obtained in these reactions are stable under ambient conditions and, hence, have been characterized with the aid of both analytical and spectroscopic methods. The composition of these products could be readily deduced from the elemental analysis values.

The absence of any absorption band at ∼2350 cm^{-1} in the Fourier transform infrared (FT-IR) spectra of **1**−**3** implies a complete reaction of P−OH groups of haloaryl phosphate ligands. Strong absorption bands observed at 1186, 1021, and 914 cm^{-1} for **1**, at 1187, 1020, and 910 cm^{-1} for **2**, and at 1187, 1020, and 909 cm^{-1} for **3** are assigned to the P═O stretching vibrations and M−O−P asymmetric and symmetric stretching frequencies, respectively. The ^{31}P NMR spectra of **1**−**3** show a single resonance at δ −5.48, −5.57, and −5.55 ppm, respectively, indicating the presence of only one type of phosphorus center in these complexes and, hence, a more symmetric structure for the products as observed previously for the complexes derived from unsubstituted monoaryl phosphate dippH$_2$.[15,17] The ^{1}H NMR spectrum of **1** shows well-separated peaks for all the protons of phosphate and collidine ligands, and their integrated intensities suggest the presence of X-dipp and collidine in a 1:1 ratio in these complexes. Two singlets observed in the aromatic region at δ 7.02 and 6.85 ppm in **1** correspond to the aryl protons of phosphate ligand and collidine, respectively. Two types of methyl protons of collidine resonate as two singlets at δ 2.34 and 2.20 ppm, while the methine and methyl protons of the isopropyl group of chloroaryl phosphate resonate as a septet and a doublet at δ 3.63 and 1.07 ppm, respectively. The ^{1}H NMR spectra of **2** and **3** are similar to that observed for **1** and, hence, are not discussed in detail here (see the Electronic Supporting Information (ESI)).

X-ray-quality single crystals of **1**−**3** were directly obtained from the reaction mixture by slow evaporation of solvent over a period of 2−3 days (see the Experimental Section). Single-crystal X-ray structure determination reveals that these compounds are isomorphous and crystallize in the tetragonal space group $I\bar{4}$. The molecular structure of **1** is shown in Figure 1,

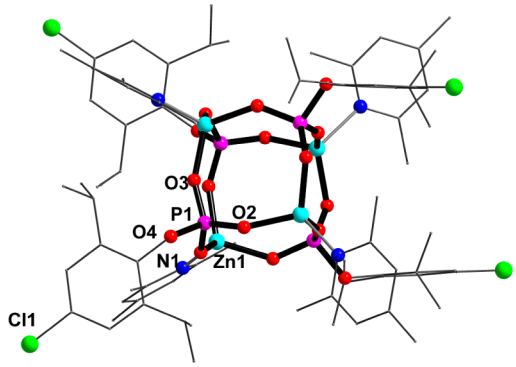

Figure 1. Molecular structure of **1** (H atoms are omitted for the sake of clarity). Selected bond distances: Zn1−O1, 1.934(2) Å; Zn1−O2, 1.927(1) Å; Zn1−O3, 1.916(3) Å; Zn1−N1, 2.079(2) Å; P1−O1, 1.525(2) Å; P1−O2, 1.509(1) Å; P1−O3, 1.493(4) Å; P1−O4, 1.626(2) Å; C4−Cl1, 1.745(2) Å. Bond angles: O−Zn−O, 95.97(2)°−118.14(3)° (ave 109.50°); O−P−O, 102.07(1)°−114.70(4)° (ave 109.26°); Zn−O−P, 125.71(4)°−155.81(5)° (ave 139.05°). For structural diagrams of **2** and **3** and their bond parameters, see the ESI.

while those of **2** and **3** are presented in the ESI. These compounds are built on a cubic framework, composed of four zinc, four haloaryl phosphate, and four collidine ligands. Zn and P atoms occupy the alternate vertices of the D4R cubic core and are bridged by O atoms in a μ_2 fashion, resulting in the formation of six nonplanar $Zn_2O_4P_2$ eight-membered rings, thereby giving it a distorted pseudo-C_4 crown conformation.

Zn centers exhibit a near ideal tetrahedral geometry with O_3N coordination environment and display an average bond angle of 109.50° for **1**, 109.84° for **2**, and 109.46° for **3**. Each of the halo-aryl phosphate ligands bridge three Zn centers in a bicapping tridentate fashion. (Harris notation for the phosphate

DOI: 10.1021/acs.inorgchem.5b00495
Inorg. Chem. 2015, 54, 4882−4894

Table 1. Comparison of Structural Parameters of Compounds 1−8, 10−12, and Some Earlier Reported D4R Zinc Phosphates

formula	crystal system	space group	Zn−N [Å]	Zn−O [Å]	P−O [Å]	Zn···P [Å]	face diagonal [Å] Zn··· Zn	face diagonal [Å] P···P	body diagonal [Å]
$[Zn(dipp)(Coll)]_4$[a]	tetragonal	$I41a$	2.087	1.916	1.532	3.196	4.419	4.632	5.529
$[Zn(dipp)(pyridine)]_4$[a]	triclinic	$\bar{P}1$	2.029	1.918	1.537	3.166	4.318	4.625	5.476
$[Zn(dipp)(2\text{-apy})]_4$[a]	monoclinic	$C2c$	2.027	1.923	1.537	3.179	4.347	4.598	5.477
$[Zn(Cl\text{-}dipp)(Coll)]_4$ (**1**)	tetragonal	$\bar{I}4$	2.079	1.921	1.491	3.197	4.471	4.527	5.536
$[Zn(Br\text{-}dipp)(Coll)]_4$ (**2**)	tetragonal	$\bar{I}4$	2.085	1.931	1.512	3.212	4.482	4.483	5.542
$[Zn(I\text{-}dipp)(Coll)]_4$ (**3**)	tetragonal	$\bar{I}4$	2.076	1.923	1.507	3.204	4.458	4.580	5.533
$[Zn(Cl\text{-}dipp)(2apy)]_4\cdot 2MeOH$ (**4**)	triclinic	$\bar{P}1$	2.020	1.933	1.511	3.175	4.447	4.541	5.544
$[Zn(Br\text{-}dipp)(2apy)]_4\cdot 2MeOH$ (**5**)	orthorhombic	$P2_12_12$	2.015	1.925	1.507	3.172	4.448	4.553	5.521
$[Zn(I\text{-}dipp)(2apy)]_4\cdot 2MeOH$ (**6**)	monoclinic	$C2/c$	2.015	1.925	1.507	3.152	4.481	4.535	5.531
$\{[Zn_4(Cl\text{-}dipp)_4(4\text{-}CNpy)_2(MeOH)_2]\cdot 2H_2O\}_n$ (**7**)	monoclinic	$P2_1/n$	2.043	1.98	1.509	3.195	4.211	4.778	
$\{[Zn_4(Br\text{-}dipp)_4(4\text{-}CNpy)_2(MeOH)_2]\cdot 2H_2O\}_n$ (**8**)	monoclinic	$P2_1/n$	2.017	2.002	1.506	3.215	4.212	4.775	
$[Zn(Cl\text{-}dipp)(Imz)]_4\cdot 2MeOH$ (**10**)	orthorhombic	$Fdd2$	1.987	1.928	1.499	3.176	4.459	4.488	5.556
$[Zn(Cl\text{-}dipp)(Phen)]_2\cdot MeOH\cdot H_2O$ (**11**)	triclinic	$\bar{P}1$	2.155	1.945	1.512	3.301	4.173	5.122	
$[Zn(dmpp)(MeOH)]_2$ (**12**)	monoclinic	$P2/c$		1.944	1.507	3.152	3.997	4.835	

[a]Data taken from ref 15.

ligand coordination: [3.111].)[18] The bond parameters found in these compounds are comparable to each other and to other reported zinc phosphates and phosphonates possessing D4R core structures (see Table 1). The average length of the P−O(M) bonds in the cubane core is 1.491 Å for **1**, 1.512 Å for **2**, and 1.507 Å for **3**. These values are significantly shorter than that of P−O single bond length (∼1.60 Å) but are considerably longer than that of P═O double bond (∼1.45−1.46 Å).[19] The average Zn−O−P bond angles along the edges of cubane are 139.05° for **1**, 139.03° for **2**, and 139.01° for **3**, and are smaller than 180°, thus rendering a spherical finish to cubic core structure. The dimensions of the cubic cores of these compounds can be understood from the Zn···P edges (3.20 Å), P···P face diagonals (4.50 Å), Zn···Zn face diagonals (4.47 Å), and Zn···P body diagonals (5.54 Å) (Table1). The adjacent molecules in the lattice are held together by van der Waals interactions, with C−X (Cl, Br, I) linkages exhibiting no hydrogen-bonding interactions.

2.2. Syntheses and Structures of 2-Aminopyridine and Halogen Decorated D4R-Zn-Cubanes 4−6. While it has been observed that the molecules of **1**−**3** do not have any secondary interactions between them to form extended structures in the solid state, an amino pyridine was used in place of collidine in order to induce intercubane hydrogen-bonding interactions. Thus, a 1:1:1 stoichiometric reaction of $[Zn(OAc)_2\cdot 2H_2O]$ and haloaryl phosphates X-dippH$_2$ in the presence of 2-aminopyridine (2-apy) in methanol at room temperature leads to the formation of halide- and amine-functionalized cubanes $[Zn(X\text{-}dipp)(2\text{-}apy)]_4\cdot 2MeOH$ (X = Cl (**4**), Br (**5**), I (**6**)) (Scheme 1). The crystalline products are stable under ambient conditions and have been characterized by analytical and spectroscopic methods. The spectral data for **4**−**6** are similar to those obtained for **1**−**3**, with, however, an exception in the ^{1}H NMR spectra for H$_b$ (ortho aromatic proton of 2-apy), which shows a significant upfield shift of ∼δ 0.5 ppm, unlike other protons of the ancillary ligand, which exhibit the expected downfield shift (see the ESI).

Single crystals of **4**−**6** suitable for diffraction studies were obtained by slow evaporation of the solvent from the reaction mixture over a period of 3−4 days at room temperature. Although the three compounds **4**−**6** crystallize in three different crystal systems (triclinic ($\bar{P}1$) for **4**, orthorhombic ($P2_12_12$) for **5**, and monoclinic ($C2/c$) for **6**), these molecules are isostructural. A perspective view of the molecular structure of **4** is shown in Figure 2 (for details of **5** and **6**; see the ESI),

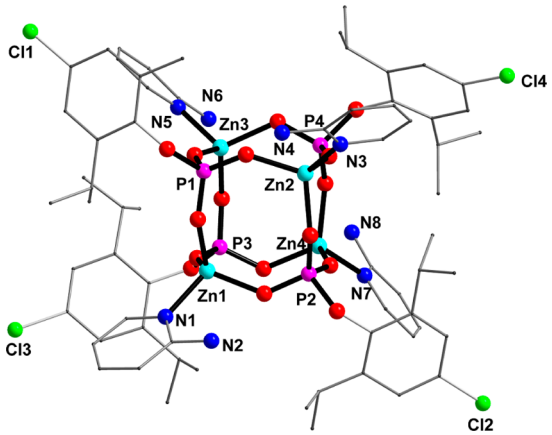

Figure 2. Molecular structure of **4**. Selected bond distances: Zn1−O2, 1.924(5) Å; Zn1−O10, 1.916(3) Å; Zn1−O6, 1.938(1) Å; Zn1−N1, 2.013(1) Å; P1−O1, 1.626(4) Å; P1−O2, 1.507(7) Å; P1−O3, 1.516(6) Å; P1−O4, 1.508(3) Å; C4−Cl1, 1.754(3) Å. Bond angles: O−Zn−O, 94.77(2)°−117.99(4)° (ave 109.50°); O−P−O, 102.07(3)°−114.70(1)° (ave 109.26°); Zn−O−P, 131.71(1)°−150.81(1)° (ave 139.05°). For structural diagrams of **5** and **6**, see the ESI.

and the supramolecular association is depicted in Figure 3. As in the case of **1**−**3**, these molecules are also built on a central cubic framework with Zn and P occupying alternate corners of the inorganic cubic core, albeit the engagement of −NH$_2$ functionalities in secondary interactions.

As described above, a [3.111] mode of coordination[18] of each phosphate ligand to three different Zn centers results in a cubic inorganic core for these compounds, whose periphery is covered by the haloaryl ring and amino-functionalized 2-apy ring. The bond parameters for **4**−**6** are essentially similar to

DOI: 10.1021/acs.inorgchem.5b00495
Inorg. Chem. 2015, 54, 4882−4894

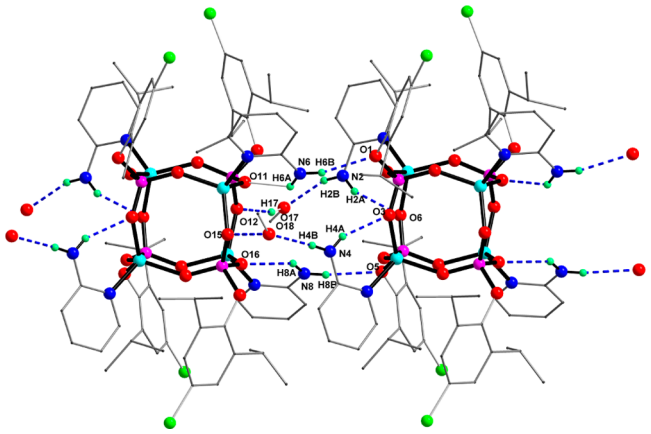

Figure 3. Intermolecular hydrogen bonding interactions in **4**, leading to the formation of a one-dimensional (1-D) polymeric supramolecular assembly in the solid state. (N2−H2A···O6, 2.921(1) Å, 132.85(2)°; N2−H2B···O17, 2.896(1) Å, 160.15(2)°; N4−H4A···O3, 2.902(1) Å, 152.83(2); N4−H4B···O18, 2.904(2) Å, 176.66(2)°; N6−H6B···O1 3.103(1) Å, 162.87(2)°; N6−H6A···O11, 3.116(1) Å, 137.14(2)°; N8−H8B···O5, 3.285(1) Å, 147.27(2)°; N8−H8A···O16, 3.187(3) Å, 145.26(2)°; O17−H17···O12, 2.837(2) Å, 176.11(2)°.)

those described for **1**−**3**, and are also comparable to other reported D4R-cubic zinc phosphates and phosphonates (Table 1).

Unlike in **1**−**3**, there is a C−H···π interaction between the hydrogen atom (H_b, ortho- to pyridinic N) and the aromatic ring of the haloaryl phosphate ligands in **4**, leading to an unexpected upfield shift of H_b proton resonance in the ^{1}H NMR spectrum (see Figure 4).

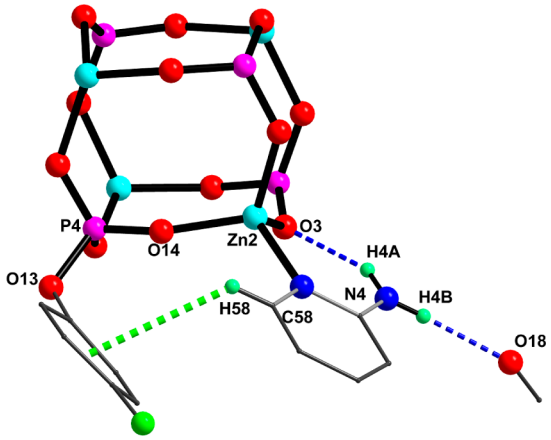

Figure 4. C−H···π interaction between hydrogen atom (ortho- to N) and the aromatic ring in **4** (C−H···π distance = 3.185(1) Å).

The presence of the amino substituent on the pyridine ring enables formation of a polymeric chain in these compounds. As it is depicted in Figure 3, in compounds **4**−**6**, all the four NH_2 groups on each molecule are involved in both intramolecular and intermolecular hydrogen bonding. The two methanol molecules in the lattice of these compounds act as hydrogen-bond acceptors as well as donors, and help in the communication of hydrogen bonding interactions of the $-NH_2$ protons of 2-apy (N4−H4B and N2−H2B) to the framework oxygen atoms (O15 and O12) of the adjacent cubane. The various hydrogen bond parameters of **4** are given in Figure 3 and for **5** and **6** in the ESI.

2.3. Formation and Structures of Square-Wave Zinc Phosphate Polymers 7−9. To further investigate the role of ancillary ligand in the chemistry of these zinc phosphates, 4-CNpy was used as ancillary ligand with the intent to study its effect on the structure of resulting phosphates in addition to functionalization of these compounds with nitrile groups, which can provide easy nucleophilic addition centers. The reaction of $[Zn(OAc)_2{\cdot}2H_2O]$ and haloaryl phosphates with 4-CNpy in methanol at room temperature in 1:1:1 stoichiometry yields zinc phosphates $[Zn_4(X\text{-dipp})_4(4\text{-CNpy})_2(MeOH)_2]{\cdot}2H_2O$ (X = Cl (**7**), Br (**8**), I (**9**)) (see Scheme 2). The crystalline products obtained are stable under ambient conditions.

The spectral data of **7**−**9** are comparable to **1**−**6**, except for the 2:1 ratio of X-dipp and 4-CNPy suggested by ^{1}H NMR spectroscopy for **7**−**9**, compared to the 1:1 ratio of phosphate and ancillary ligands in **1**−**6** (see the ESI). The observation from the ^{1}H NMR spectroscopy of **7**−**9** that, for every two phosphate ligands in the molecule, there is only one cyanopyridine co-ligand (in other words, the cyanopyridine ligands are coordinated to only half the number of Zn centers) indicated that the molecular structures of these compounds should be significantly different from the cubane architecture present in compounds **1**−**6**. Hence, structure determination for **7** and **8** has been undertaken.

Diffraction-quality single crystals of **7** and **8** have been obtained from the reaction mixture by slow evaporation of the solvent over a period of 2 weeks. Single-crystal X-ray structure determination reveals that these compounds are isomorphous and crystallize in the monoclinic $P2_1/n$ space group. A perspective view of the molecular structure of **7** is shown in Figure 5 (for **8**, see the ESI). Compounds **7** and **8** are 1-D polymers, which could have presumably formed by *side-by-side* bridging of S4R SBUs along one of the edges (see below). Each building unit of **7** and **8** consists of four Zn atoms, four haloaryl phosphates, two 4-CNpy, and two molecules of methanol, besides the presence of two water molecules in the lattice. The Zn and P centers occupy alternate vertices of the S4R building units and are bridged by the O atoms in a μ_2 fashion. The two Zn centers in the asymmetric unit of **7** and **8** are chemically nonequivalent, because, besides being coordinated by three O atoms from three different phosphate ligands, Zn1 is capped by 4-CNpy while a methanol molecule occupies the fourth coordination site on Zn2. Zn centers in both of these molecules exhibit a tetrahedral coordination geometry with an average bond angle of 109.11° and 109.23° for Zn1 and 109.21° and 109.09° for Zn2 in **7** and **8**, respectively. Each of the haloaryl phosphate ligands bridge three Zn centers in a tridentate fashion (Harris notation [3.111]).[18] The average length of P−O(M) bond in cyclic core is 1.515 Å and 1.513 Å in **7** and **8**, respectively. These values are significantly shorter than that of P−O single bond length (∼1.60 Å) but considerably longer than that of the P═O double bond (∼1.45−1.46 Å).[19]

Compounds **7** and **8** represent a new class of 1-D polymers resulting from side-by-side fusion of S4R rings in the form of square wave polymers, a structural modification previously unknown in metal phosphate chemistry. The polymeric assembly of **7** and **8** consist of S4R SBUs, labeled as type "A" (which undergo sidewise condensation of their edges, forming Zn−O−P bonds) and two new type of S4R rings, labeled as typea "B" and 'C" (Figure 6). The three types of S4R rings in these molecules arrange in ABAC manner. The "A" ring consists of Zn1, Zn2, P1, and P2 vertices with a Zn1−Zn2 diagonal of 4.205(1) Å, and a P1−P2 diagonal of 4.667(1) Å;

DOI: 10.1021/acs.inorgchem.5b00495
Inorg. Chem. 2015, 54, 4882−4894

Scheme 2. Synthesis of 7−9

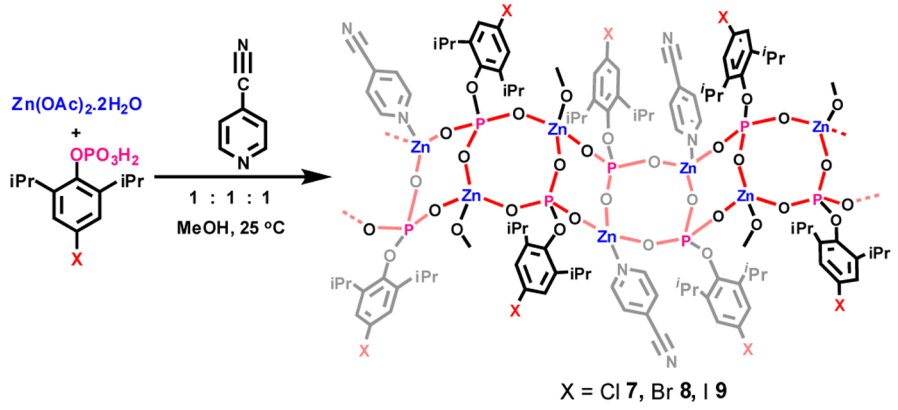

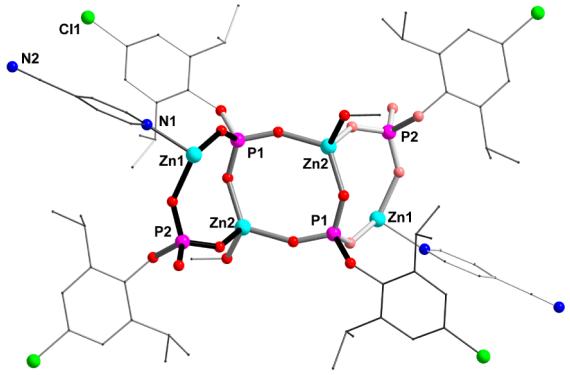

Figure 5. Molecular structure of a fragment of polymeric **7** (H atoms are omitted for the sake of clarity). Selected bond distances: Zn1−O2, 1.910(3) Å; Zn1−O6, 1.890(1) Å; Zn1−O4, 1.896(7) Å; Zn1−N1, 2.403(1) Å; Zn2−O4, 1.896(7) Å; Zn2−O7, 1.908(3) Å; Zn2−O3, 1.903(1) Å; P1−O2, 1.513(1) Å; P1−O3, 1.497(0) Å; P1−O4, 1.492(4) Å; P2−O7, 1.496(3) Å; P2−O6, 1.4999(1) Å. Bond angles: Zn1−O6−P2, 141.16(0)°; Zn1−O2−P1, 138.52(2)°; Zn2−O7−P2, 134.47(2)°; Zn2−O3−P1, 134.03(0)°; Zn2−O4−P1, 153.04(1)°. For **8**, see the ESI.

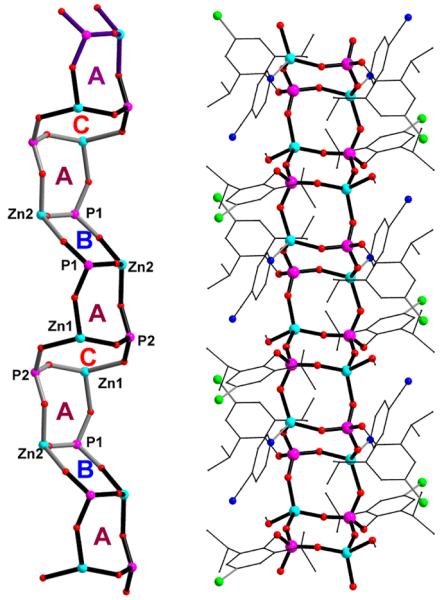

Figure 6. Polymeric structure of **7**: (a) "A" type rings bridge through their edges, forming "B" and "C" type rings, which arrange in ABAC order; (b) square wave shaped inorganic core of **7**, covered by organic ligands. (H atoms are omitted for the sake of clarity.)

the Zn−P edge distances range from 3.133(1) Å to 3.205(2) Å and the Zn−O−P bond angles range from 134.06(1)° to 141.15(2)° in **7**. The "B" ring consists of two Zn2 and two P1 vertices with a Zn2···Zn2 diagonal of 4.244(2) Å and a P1···P1 diagonal of 4.832(1) Å; the Zn···P edge distances range from 3.133(1) Å to 3.296(2) Å and the Zn−O−P bond angles range from 134.06(1)° to 153.07(3)°. However, the "C" ring consists of two Zn1 and two P2 centers with a Zn1···Zn1 diagonal of 4.542(1) Å and a P2···P2 diagonal of 4.336(1) Å; the Zn···P edge lengths range from 3.079(1) Å to 3.199(2) Å and the Zn−O−P bond angles range from 127.14(1)°−141.167(3)°, respectively. Bond angles and distances for compound **8** are similar to **7** (see the ESI). The water molecules in the lattice of **7** and **8** undergo hydrogen bonding by acting as an acceptor for methanol molecule coordinated to Zn centers and a donor for one of the framework O atoms.

2.4. Synthetic Strategies to S4R Zinc Phosphates and Isolation of Supramolecular D4R 10 and a Discrete S4R Zinc Phosphate (11). The fact that the complexes **1**−**9** are essentially built by the fusion of S4R units, an attempt has been made to isolate stable S4R structures that do not associate to form larger structures. Since the association of S4R rings primarily takes place because of the coordinative association at the Zn centers, the reaction of zinc acetate with monoaryl phosphates were carried out in the presence of large excess of a less bulky ancillary ligand such as imidazole (Imz) and also by the addition of a chelating ligand such as 1,10-phenanthroline (1,10-phen). The former reaction involving imidazole does not lead to isolation of the desired S4R product, but results in the quantitative isolation of the familiar D4R phosphate $[Zn(Cl\text{-}dipp)(Imz)]_4{\cdot}2MeOH$ (**10**) and the unconsumed imidazole ligand. (See Scheme 3.) However, the reaction involving 1,10-phenanthroline smoothly proceeds to yield the desired neutral S4R zinc phosphate $[Zn(Cl\text{-}dipp)(1,10\text{-}phen)(H_2O)]_2{\cdot}MeOH{\cdot}H_2O$ (**11**).

The FT-IR and nuclear magnetic resonance (NMR) (^1H and ^{31}P) spectroscopic features of **10** are very similar to the other D4R zinc phosphates **1**−**6** described above (see the ESI). The spectral data of **11** are comparable to zinc phosphates **1**−**10** (see the ESI). Single-crystal structure determination of **10** further confirms its structural similarities to **1**−**6** (Figure 7, Table 1). However, compound **10** differs from compounds **1**−**6** in aggregation behavior arising due to hydrogen-bonding interactions. Compound **10** undergoes intermolecular hydrogen bonding between imidazole N−H (N2−H2 and N4−H4)

DOI: 10.1021/acs.inorgchem.5b00495
Inorg. Chem. 2015, 54, 4882−4894

Scheme 3. Strategies To Isolate S4R Leading to the Isolation of D4R (10) and S4R (11)

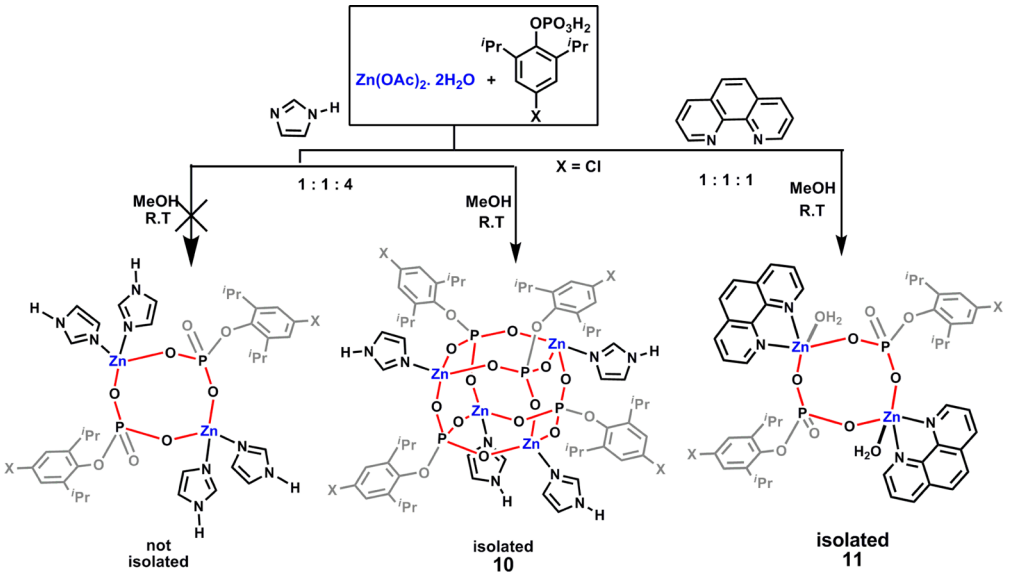

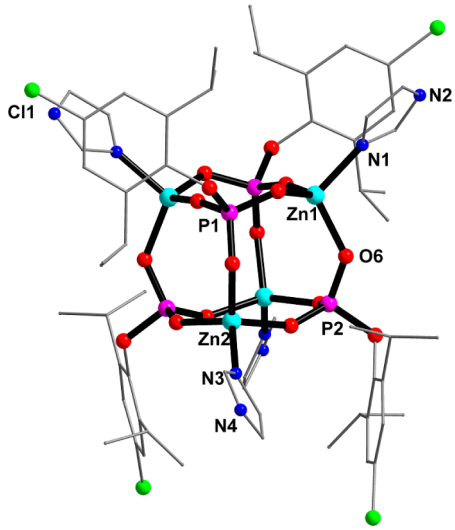

Figure 7. Molecular structure diagram of **10**. Selected bond distances: Zn1−O2, 1.906(3) Å; Zn1−O6, 1.951(1) Å; Zn1−O4, 1.948(7) Å; Zn1−N1, 1.987(1) Å; P1−O2, 1.495(1) Å; P1−O3, 1.499(0) Å; P1−O4, 1.519(4) Å. Bond angles: Zn1−O6−P2, 131.65(0)°; Zn1−O2−P1, 163.79(2)°; Zn2−O4−P1, 124.45(2)°.

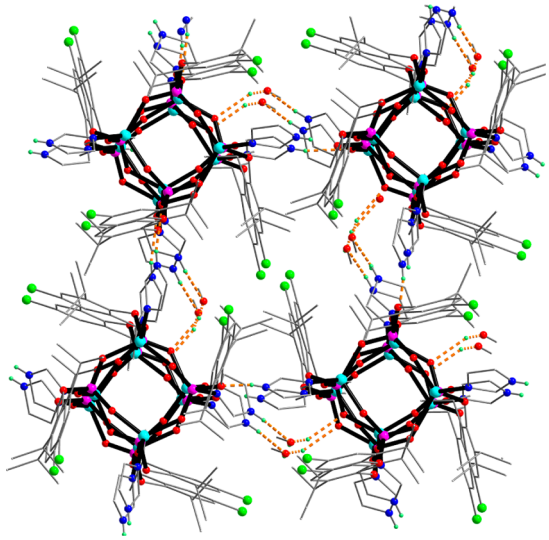

Figure 8. Three-dimensional (3-D) supramolecular assembly formation through hydrogen bonding in **10**. (Bond distances and angles: O4···H9−O9, 2.804(2) Å, 154.34(2)°; O9···H2−N2, 2.791(2) Å, 171.97(2)°; and O4···H6−N6, 2.856(1) Å, 168.21(2)°.)

and framework O atoms (O4 and O6), with the help of methanol molecules in the lattice leading to the formation of a 3-D supramolecular assembly (see Figure 8).

X-ray-quality single crystals of **11** (triclinic, $P\bar{1}$) have been obtained directly by slow evaporation of solvent from the reaction mixture at room temperature. A perspective view of the molecular structure of **11** is shown in Figure 9. Compound **11** is a cyclic zinc phosphate that exists as a rare neutral S4R metal phosphate. The asymmetric unit of the unit **11** consists of one-half of the cyclic phosphate which is composed of one Zn, one phosphate, one 1,10-phenanthroline, and one molecule of coordinated water, one lattice methanol, and one lattice water. The core of **11** is a $Zn_2O_4P_2$ eight-membered ring that exists in an almost planar conformation, presumably because of a trigonal bipyramidal geometry around the Zn centers. However, the S4R fragments in **1**−**6** exist in a pseudo-C_4 crown conformation (see Figure 9).

Each of the Zn centers in **11** is in a trigonal bipyramidal coordination environment provided by two phosphate O atoms (from two different phosphate ligands which exhibit a [2.110] mode of coordination[18]), a chelating 1,10-phenanthroline, and a water molecule. P centers are in a tetrahedral environment with an average bond angle of 109.44°. Because of steric hindrance, as well as sufficient coordination saturation at the Zn, provided by 1,10-phen and water, the phosphoryl P═O group remains free in the phosphate ligands. The P−O(Zn) bond lengths are 1.501(2) and 1.506(1) Å, while the Zn−O−P bond angle values are 134.66(5)° and 166.67(2)°. The Zn···Zn and P···P diagonal distances in **11** are 4.173(2) and 5.122(8) Å, respectively. The two P═O as well as two coordinated water molecules are in trans configuration about the plane of S4R ring.

Assisted by the presence of water in the lattice and the free phosphoryl P═O groups, **11** undergoes intermolecular

DOI: 10.1021/acs.inorgchem.5b00495
Inorg. Chem. 2015, 54, 4882−4894

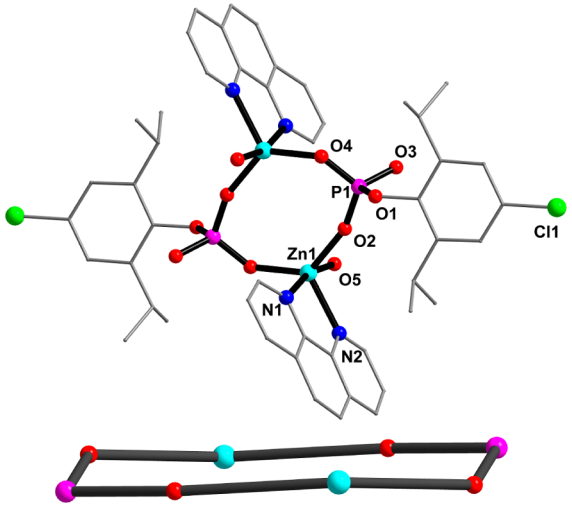

Figure 9. (Top) Molecular structure of **11**. Selected bond distances: Zn1−O2, 1.945(3) Å; Zn1−O4, 1.945(5) Å; Zn1−N1, 2.194(5) Å; Zn1−N2, 2.122(3) Å; P1−O2, 1.501(2) Å; P1−O3, 1.512(9) Å; P1−O4, 1.526(4) Å. Bond angles: Zn1−O4−P1, 134.66(5)°; Zn1−O2−P1, 160.67(2)°; N1−Zn1−N2, 77.86(2)°. (Bottom) S4R ring of **11**, showing an almost planar configuration; Zn1, P1, O2 and O4 deviate by 0.088, 0.094, 0.012, and 0.134 Å, respectively, from the mean plane.

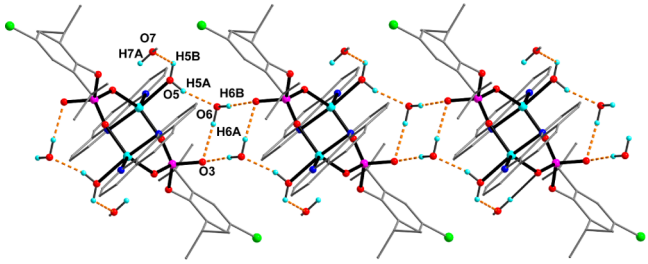

Figure 10. Lattice water molecules mediated hydrogen bonding, leading to the formation of a 1-D chain in **11**. (O3···H6A−O6, 2.820(2) Å, 170.47(2)°; O3···H6B−O6, 2.706(1) Å, 167.45(2)°; O6···H5A−O5, 2.679(1) Å, 163.55(2)°.)

hydrogen bonding to form a hydrogen-bonded 1-D polymer (Figure 10). Each lattice water forms three hydrogen bonds, acting as a donor for two P═O atoms (O6−H6A···O3 and O6−H6B···O3) and as an acceptor for the coordinated water molecule (O5−H5A···O6), (Figure 10). The methanol molecules in the lattice are also involved in the formation of terminal hydrogen bond with coordinated water molecule (O5−H5B···O7). The hydrogen-bonded 1-D chains are further associated into two-dimensional (2-D) sheets through $\pi-\pi$ interactions involving the aryl rings of phenanthroline ($\pi-\pi$/C−C distances range: 4.012−4.256 Å) (see Figure 11).

2.5. Synthesis and Structure of Zigzag Zinc Phosphate Polymer {[Zn(dmpp)(MeOH)]$_4$}$_n$ (12). The reactions leading to the formation of products **1**−**11** have essentially been controlled by the ancillary ligands used, such as collidine, 2-aminopyridine, 4-cyanopyridine, imidazole and 1,10-phenanthroline, paying much less attention to the role played the phosphate ligand itself, in terms of the steric control and also the source of Zn ion. For example, the X-dippH$_2$ ligands used to obtain **1**−**11** contain bulky isopropyl substituents on the ortho positions of the aryl ring. An obvious question to address would be what happens if this bulkiness is completely removed or at least reduced by placing hydrogen or methyl groups as the

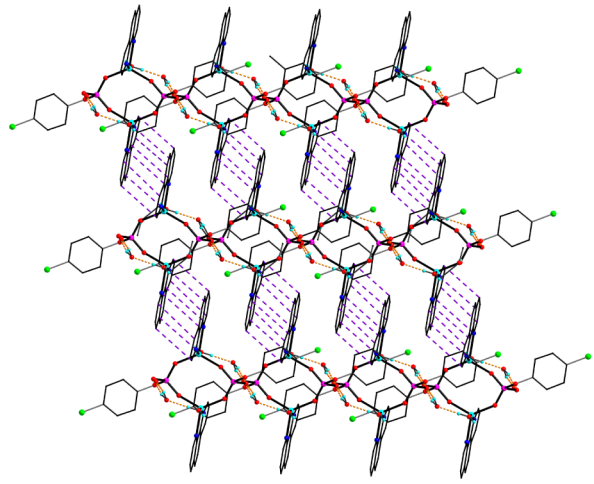

Figure 11. Interchain $\pi-\pi$ stacking between 1,10-phenanthroline groups of adjacent polymeric chains in **11**, resulting in two-dimensional (2-D) assemblies. (H atoms and isopropyl groups of phosphate ligand are omitted for the sake of clarity; $\pi-\pi$/C−C = 4.012−4.256 Å.)

ortho substituent. Similarly, a covalent source of zinc (zinc acetate) has been used in all the above-described reactions, and it would be interesting to investigate whether an ionic salt source of zinc such as zinc nitrate or perchlorate would lead to a zinc phosphate with a different architecture. A third variation in these reactions could be to completely avoid using a pyridinic ancillary ligand.

To evaluate these possibilities, a triple change was introduced by (a) replacing X-dippH$_2$ by 2,6-dimethylphenyl phosphate (dmppH$_2$), (b) replacing zinc acetate by zinc nitrate hexahydrate, and (c) replacing pyridinc ancillary ligand just by solvent methanol, as shown in Scheme 4, to obtain a crystalline zinc

Scheme 4. Synthesis of Zigzag Polymer 12

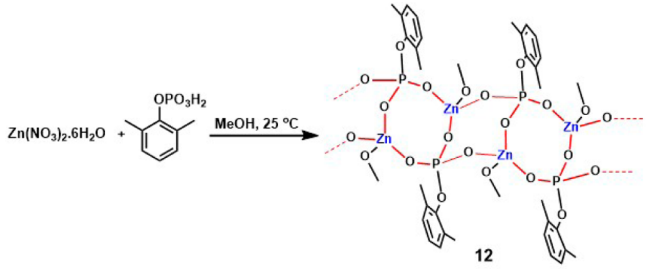

phosphate polymer of the composition {[Zn(dmpp)(MeOH)]$_4$}$_n$ (**12**). Compound **12** has been characterized using analytical and spectroscopic methods. The complexation of dmppH$_2$ to zinc is supported by presence of sharp absorption bands at 1116 and 929 cm^{-1} in the FT-IR spectrum, which indicate the presence of P−O−Zn linkages in the product. The ^{31}P NMR spectrum shows a single resonance at δ −4.2 ppm, suggesting a symmetric structure for **11**. The ^{1}H NMR spectrum shows a set of two multiplets at ∼7.0 ppm and a singlet at 2.10 ppm, corresponding to the aryl C−H and methyl protons of the phosphate ligand, respectively.

Crystal structure analysis of **12** (monoclinic *P*2/*c*) revealed that it is a 1-D polymer that has been formed by a lateral (*edge-to-edge*) fusion of S4R rings. The asymmetric unit of **12** consists of one Zn ion, one dimethylphenyl phosphate, and a coordinated methanol (see Figure 12). The Zn center in **12**

DOI: 10.1021/acs.inorgchem.5b00495
Inorg. Chem. 2015, 54, 4882−4894

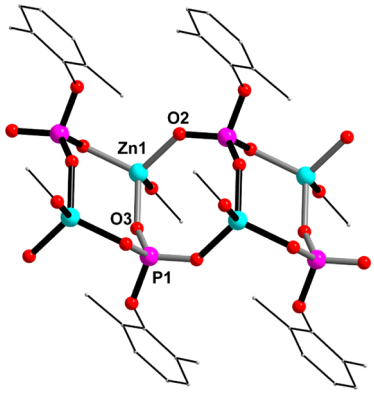

Figure 12. Molecular structure diagram of a section of polymeric **12**. Selected bond distances: Zn1−O2, 1.903(3) Å; Zn1−O3, 1.901(1) Å; Zn1−O4, 1.944(7) Å; P1−O2, 1.507(1) Å; P1−O4, 1.531(0) Å; P1−O4, 1.531(4) Å. Bond angles: Zn1−O4−P1, 119.79(2)°; Zn1−O3−P1, 146.34(2)°.

exhibits a tetrahedral environment (average bond angle = 109.15°), as is the P center (average bond angle = 109.05°). The aryl phosphate ligand bridges three different zinc centers in a tridentate fashion with [3.111] mode of coordination.[18] The average P−O(M) bond length in the cyclic core of **12** is 1.512 Å, which represents a value in between P−O single and P═O double bond distances.[19]

Unlike polymers **6** and **7**, which are square wave polymers, the polymeric backbone **12** resembles a zigzag chain, which is presumably formed via the *edge-to-edge* fusion of a series of trans S4R units. Unlike the ABAC type of arrangement of S4R rings in **7** and **8**, S4R rings in **12** arrange in an ABAB manner (see Figure 13 and Scheme 5, presented later in this work). "A"

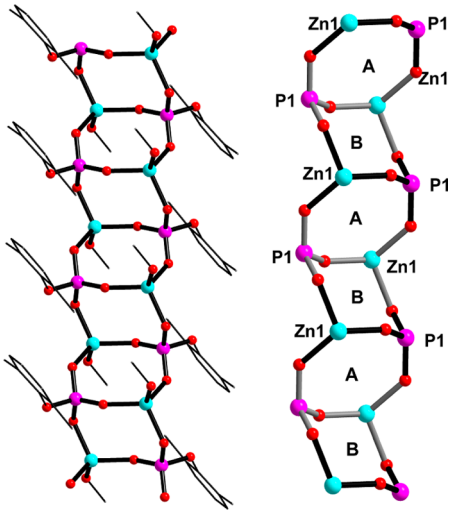

Figure 13. A perspective view (left) and the backbone architecture (right) of polymeric zinc phosphate (**12**).

type rings have a Zn···Zn diagonal distance of 4.445(1) Å, a P···P diagonal distance of 4.588(1) Å, a Zn···P edge distance of 3.131(1)-3.255(2) Å, and Zn−O−P bond angles of 132.93(1)°−146.34(2)°. The "B" type rings have a Zn···Zn diagonal of 3.997(1) Å, a P1···P1 diagonal of 4.835(1) Å, Zn···P edge distance of 3.013(1)−3.255(2) Å and Zn−O−P bond angles of 119.79(1)−146.34(3)°.

2.6. Thermal Decomposition Studies of 1−12. Thermogravimetric analysis (TGA) for the zinc phosphates **1−12** were carried out in the temperature range of 30−1200 °C under a stream of nitrogen gas at a heating rate of 10 °C min^{-1}. Compounds **1−12** are stable up to 300 °C, except for the loss of lattice solvent molecules, and show a sharp weight loss of ∼60% (compound **12** shows a loss of 43%) due to burning of organic ligands, thereby leaving behind [$ZnO_3P(OH)$], which further undergoes a loss of water molecule in the region of 500−900 °C to form zinc pyrophosphate $Zn_2P_2O_7$. Further heating of these compounds leads to the decomposition of pyrophosphates leaving behind metal oxides (ESI).

2.7. Photophysical Studies. The absorption and emission studies of 10^{-6} M solutions of **4−6** have been carried out in acetonitrile. Because of poor solubility in acetonitrile, the absorption and emission studies for compounds **1−3**, **7−9**, and **10−12** could not be performed in any solvent other than dimethylsulfoxide (DMSO), in which it was found that the DMSO molecules replace the ancillary ligands on zinc centers. Compounds **4−6**, bearing auxochrome $-NH_2$ on the ancillary ligand 2-apy, show absorption bands at 300 and 225 nm, which can be assigned to $\pi-\pi^*$ and $n-\pi^*$ transitions, respectively. However, these compounds show broad emission spectra at ∼235 nm, which represents bathochromic shift of ∼30 nm, compared to free ligands (see Figure 14 and the ESI). When

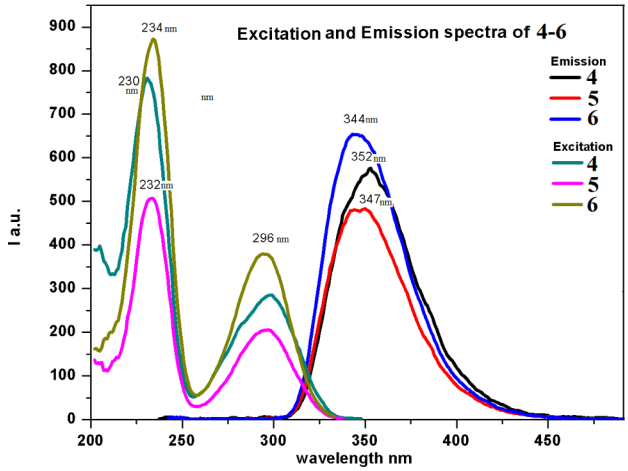

Figure 14. Emission (λ_{ex} = 225 and 300 nm) and excitation spectra for compounds **4−6** ($C = 10^{-6}$ M) in acetonitrile.

compared to free ligands, cubanes **4−6** exhibit enhanced excitation and emission intensities (see the ESI).

3. DISCUSSION

The original objective of the present work was to introduce functional groups on all eight vertices of the D4R cubanes by suitable ligand architecture for the preparation's 8-node connected framework solids. 4-Haloaryl phosphate ligands were introduced in the zinc phosphate chemistry for this purpose, with the reasoning that it is possible to form D4R cubanes on which four of the vertices will contain coordinatively unsaturated Zn centers and the other four vertices will bear reactive C−X groups. A combination of use of ditopic spacers on the zinc vertices and C−C bond formation reactions on the phosphate aryl substitutents on such D4R cubanes should lead to extended porous solids, which are assembled through both covalent and coordinate linkages simultaneously.

DOI: 10.1021/acs.inorgchem.5b00495
Inorg. Chem. 2015, 54, 4882−4894

Scheme 5. Possible Growth Pathways for the Oligomerization or Polymerization of S4R Building Units

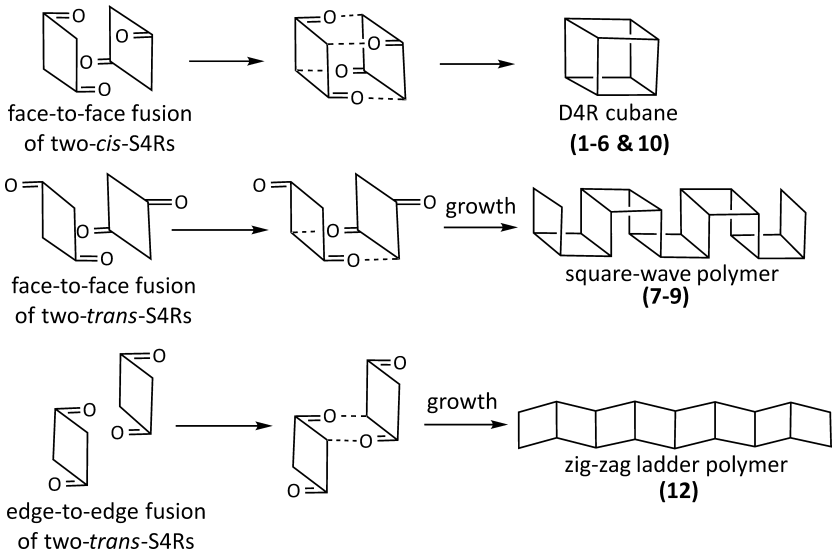

The experiments performed along these lines by the reacting the 4-haloaryl phosphates, X-dippH_2, with zinc acetate in the presence of either collidine or 2-aminopyridine yielded D4R cubanes **1**−**6** and **10**, as expected. Prior to attempting C−C bond forming reactions at the four C−X terminals, the scope of introducing other types of pyridine ligands at the zinc vertices of the D4R cubane were investigated, which led to refocusing of the present investigation.

The introduction of 4-cyanopyridine, instead of collidine or 2-aminpyridine, sprung a surprise through the isolation zinc phosphates **7**−**9**, which do not possess a D4R core. Structural investigation further revealed that the zinc phosphate core in **7**−**9** is a previously unknown square-wave type polymer, in which S4R rings are joined together sideways to produce this rather unusual architecture, instead of resulting in a simple zigzag or ladder type of polymer that has been implicated earlier in aluminophosphates and other extended metal phosphates.[9,14] The synthesis of a ladder type/zigzag polymer was finally achieved through the isolation of **12** by changing the metal source (to zinc nitrate), reducing the steric bulkiness on the arylphosphate, and also avoiding the use of a pyridinic ligand as the capping ligand.

The molecular structure determination of D4R (**1**−**6** and **10**) and polymeric (**7**−**9** and **12**) zinc phosphates divulged that both of these structural types essentially are formed from S4R building blocks, which assemble in different ways during the progress of the reaction. This led to the following question: why have the several variations introduced in the starting materials and reaction conditions failed to produce a S4R zinc phosphate? The origin of spontaneous oligomerization/polymerization, in preference to the isolation of S4R, essentially arises from the simultaneous presence of coordinative unsaturation at the Zn center and the presence of uncoordinated oxygen at the phosphate. Hence, any attempt to isolate S4R zinc phosphate should compensate for the unsaturation or provide enough steric hindrance at the metal center. The use of two equivalents of imidazole still resulted in the isolation of the D4R phosphate (**10**). However, the bulky chelate ligand, 1,10-phenanthroline, provides enough steric congestion at each Zn center, leading to the isolation of stable zinc phosphate **11** with S4R architecture, instead of allowing the polymerization/extension of these building units. The isolation of **11** thus supports the existence of S4R formation at the early stages of any other reactions described above, which is also consistent with the solution studies reported earlier.[14b]

The structure of the final product isolated in each of these reactions should then be dependent on the S4R ring conformation, the relative orientation of the free P═O groups on the ring (cis or trans), and the line of approach of S4R rings during polymerization. Scheme 5 summarizes the possible assembly pathways through which S4R rings can form these products. Presumably, when two S4R rings with cis-configuration come together and undergo *face-to-face* fusion, D4R cubanes are obtained (see Scheme 5, top). The S4R rings with trans-configuration of P═O groups can fuse in two possibly ways to form two types of polymeric chains: (i) *face-to-face* fusion of two trans-S4R units, leading to the formation of square wave polymers (**7**−**9**) (Scheme 5, middle) and (ii) *edge-to-edge* fusion of two trans-S4R units, forming zigzag-type polymers (**12**) (Scheme 5, bottom).

4. CONCLUSIONS

Structural modulations in zinc phosphate chemistry, dictated by choice of ancillary ligand have been demonstrated. Molecular zinc phosphates with D4R inorganic core are obtained by reaction of zinc acetate and 4-haloaryl phosphate with ancillary ligands collidine (**1**−**3**) or 2-apy (**4**−**6**) or imidazole (**10**). However, the ancillary ligand 4-CNpy modifies the architecture of inorganic core in these complexes significantly to form square wave one-dimensional (1-D) polymers (**7**−**9**). Furthermore, it has been observed that the reaction of zinc nitrate with sterically less demanding 2,6-dimethylphenyl phosphate yields a *zigzag*-type 1-D polymer (**12**). The structural investigations of all these zinc phosphate reveal that the S4R units are common building blocks in these structural types. This observation has been validated by isolation of neutral S4R compound **11** from the identical reaction conditions with chelating ancillary ligand 1,10-phenanthroline, which provides necessary coordination saturation at the Zn center to avoid further aggregation.

Finally, the isolation of four different structural types of zinc phosphates from seemingly similar starting materials and

DOI: 10.1021/acs.inorgchem.5b00495
Inorg. Chem. 2015, 54, 4882−4894

reaction conditions reveals that the overall energy landscape of such reaction should contain several minima of comparable energies. However, these products may have very different architectures. Hence, it would be of interest and relevance to quantify the energetics associated with these oligomerization and polymerization reactions of the S4R building block, using suitable computational models at appropriate levels of theory. We are currently investigating these aspects.

5. EXPERIMENTAL SECTION

5.1. Methods and Materials. All the compounds reported in the present study are stable under ambient conditions; hence, no particular precautions were taken during their synthesis. The melting points were measured in glass capillaries and are reported uncorrected. Infrared spectra were obtained on a Perkin−Elmer Spectrum One FT-IR spectrometer with KBr diluted disks. Microanalyses were performed on a microanalyzer (Thermo Finnigan, Model FLASH EA 1112). The ^{1}H (Me_4Si internal standard) and ^{31}P (85% H_3PO_4 external standard) NMR spectra were recorded using a Bruker 400 and 500 MHz spectrometer. Thermogravimetric analysis (TGA) study was carried out on a Perkin−Elmer Pyris thermal analysis system under a stream of nitrogen gas at the heating rate of 10 °C/min. The ESI-MS studies were carried out on Bruker MaXis impact mass spectrometer.

Solvents were purified according to standard procedures prior to use.[20] Commercially available starting materials such as $[Zn(OAc)_2{\cdot}2H_2O]$ (s.d. Fine), $[Zn(NO_3)_2{\cdot}6H_2O]$ (s.d Fine), 2-amino pyridine (Lancaster), collidine (Lancaster), 4-cyano pyridine (Lancaster), and 1,10-phenanthroline were used as procured. The ligands 4-chloro-2,6-di*iso*propylphenyl phosphate, 4-bromo-2,6-di*iso*propylphenyl phosphate, and 4-iodo-2,6-diisopropylphenyl phosphate have been synthesized as reported in the literature.[16]

5.2. Synthesis of 1−3. A solution of X-dippH_2 (X = Cl 0.073 g, Br 0.084 g, I 0.096 g, 0.25 mmol) and $[Zn(OAc)_2{\cdot}2H_2O]$ (0.055 g, 0.25 mmol) in methanol (30 mL) was stirred until it became clear and then collidine (0.030 g, 0.25 mmol) was added dropwise via a syringe. The reaction mixture was filtered and kept for 3−4 days, to yield crystals of **1**−**3**.

1. Yield: 0.35 g (72%). Melting point (Mp): >250 °C. Anal. Calcd for $C_{80}H_{108}N_4Cl_4O_{16}P_4Zn_4$ (M_r = 1909.1): C, 50.33; H, 5.70; N, 2.93. Found: C, 49.82; H, 5.61; N, 3.71. FT-IR (KBr, cm^{-1}): 2967 (s), 2867 (m), 1624 (s), 1574 (w), 1455 (m), 1388 (w), 1186 (s), 1021 (s), 914 (w), 822 (s), 688 (w), 543 (w). ^{1}H NMR (DMSO-d_6, 400 MHz) δ 7.02 (s, 8H, Ar), 6.85 (s, 8H, Ar-collidine), 3.63 (septet, $^{3}J_{H-H}$ = 6.8 Hz, 8H, ^{i}Pr-CH), 2.35 (s, 24H, *o*-CH_3-collidine), 2.21 (s, 12H, *p*-CH_3-collidine), 1.09 (d, $^{3}J_{H-H}$ = 6.8 Hz, 48H, ^{i}Pr−CH_3) ppm. ^{31}P NMR (DMSO-d_6, 161 MHz): δ −5.4 ppm. TGA: temperature range (weight loss): 30−200 °C (∼2.5%); 200−400 °C (∼62.0%); 400−500 °C (∼3.5%); 500−900 °C (∼1.5%). ESI-MS: *m*/*z* calc. for [{Zn(Cl-dipp)(coll)}$_4$]: 1909.1630; found 1909.2213 [M]$^+$.

2. Yield: 0.38 g (72%). Mp: >250 °C. Anal. Calcd for $C_{80}H_{108}N_4Br_4O_{16}P_4Zn_4$ (M_r = 2086.8): C, 46.04; H, 5.22; N, 2.68. Found: C, 45.81; H, 4.98; N, 3.18. FT-IR (KBr, cm^{-1}): 2967 (s), 2868 (m), 1624 (s), 1572 (w), 1452 (m), 1382 (w), 1187 (s), 1020 (s), 910 (w), 800 (s), 683 (w), 539 (w). ^{1}H NMR (DMSO-d_6, 400 MHz): δ 7.13 (s, 8H, Ar), 6.83 (s, 8H, Ar-collidine), 3.62 (m, $^{3}J_{H-H}$ = 6.8 Hz, 8H, ^{i}Pr-CH), 2.33 (s, 24H, *o*-CH_3-collidine), 2.19 (s, 12H, *p*-CH_3-collidine), 1.07 (d, $^{3}J_{H-H}$ = 6.8 Hz, 48H, ^{i}Pr−CH_3) ppm. ^{31}P NMR (DMSO-d_6, 161 MHz): δ −5.5. TGA: temperature range (weight loss): 30−260 °C (1.8%); 260−350 °C (∼40.5%); 350−500 °C (21.0%); 500−850 °C (∼5.5%); 850−1050 °C (∼14.5%). ESI-MS: *m*/*z* calc. for [{Zn(Br-dipp)(coll)}$_4$] 2086.8574; found 2087.0095 [M+H]$^+$.

3. Yield: 0.39 g (68.0%). Mp: >250 °C. Anal. Calcd for $C_{80}H_{108}N_4I_4O_{16}P_4Zn_4$ (M_r = 2274.0): C, 42.24; H, 4.79; N, 2.46. Found: C, 41.92; H, 4.89; N, 2.42. FT-IR (KBr, cm^{-1}): 2967 (s), 2866 (m), 1624 (s), 1569 (w), 1442 (m), 1337 (s), 1187 (s), 1020 (s), 909 (w), 790 (m), 772 (m), 678 (w), 538 (w). ^{1}H NMR (DMSO-d_6, 400 MHz): δ 7.28 (s, 8H, Ar), 6.88 (s, 8H, Ar-collidine), 3.62 (m, $^{3}J_{H-H}$ = 6.8 Hz, 8H, ^{i}Pr-CH), 2.35 (s, 24H, *o*-CH_3-collidine), 2.21 (s, 12H, *p*-CH_3-collidine), 1.06 (d, $^{3}J_{H-H}$ = 6.8 Hz, 48H, ^{i}Pr−CH_3) ppm. ^{31}P NMR (DMSO-d_6, 161 MHz): δ −5.5 ppm. TGA: temperature range (weight loss): 30−200 °C (1.9%); 200−400 °C (∼64.5%); 400−600 °C (∼5.0%); 600−870 °C (∼1.5%). ESI-MS: *m*/*z* calc. for [{Zn(I-dipp)(coll)}$_4$] 2274.0060; found 2275.9564 [M+H]$^+$.

5.3. Synthesis of 4−6. A solution of X-dippH_2 (X = Cl 0.073 g, Br 0.084 g, I 0.096 g, 0.25 mmol) and $[Zn(OAc)_2{\cdot}2H_2O]$ (0.055 g, 0.25 mmol) in methanol (30 mL) was stirred until it became clear, and then a solution of 2-apy (0.023 g, 0.25 mmol) in methanol (15 mL) was added slowly to give a clear solution. The resulting solution was filtered and kept for 3−4 days to yield crystals of **4**−**6**.

4. Yield: 0.30 g (66%). Mp: > 250 °C. Anal. Calcd for $C_{70}H_{96}Cl_4N_8O_{18}P_4Zn_4$ (M_r =1856.2): C, 45.08; H, 5.19; N, 6.01. Found: C, 45.16; H, 4.95; N, 6.05. FT-IR (KBr, cm^{-1}): 3462 (m), 3362 (m), 3223 (w), 2870 (w), 1638 (s) 1567 (w), 1448 (s), 1452 (s), 1337(s), 1186 (s), 1021 (s), 918 (w), 827 (m), 773 (m), 796 (w), 547 (w). ^{1}H NMR (DMSO-d_6, 400 MHz): δ 7.51−7.47 (t, $^{3}J_{HH}$ = 7.1 Hz, 4H, Pyr), 7.42 (br, 4H, pyr), 6.98 (s, 8H, Ar), 6.59−6.57 (d, $^{3}J_{HH}$ = 8.3 Hz, 4H, Pyr), 6.41−6.44 (t, $^{3}J_{HH}$ = 6.2 Hz, 4H, Pyr), 6.32 (br, 8H, NH_2), 3.56 (m, $^{3}J_{H-H}$ = 6.8 Hz, 8H, ^{i}Pr−CH), 0.98 (d, $^{3}J_{H-H}$ = 6.8 Hz, 48H, CH_3) ppm. ^{31}P NMR (DMSO-d_6, 161 MHz): δ −5.6 ppm. TGA: temperature range (weight loss): 30−200 °C (∼2.0%); 200−400 °C (∼64.5%); 400−600 °C (∼5.0%); 600−870 °C (∼1.5%). ESI-MS: *m*/*z* calc. for [{Zn(Cl-dipp)(2apy)}$_4$·2MeOH] 1856.2182; found 1801.1048 [M−2MeOH+H]$^+$.

5. Yield: 0.35 g (69%). Mp: >290 °C. Anal. Calcd for $C_{70}H_{96}N_8Br_4O_{18}P_4Zn_4$, ($M_r$ = 2042.5): C, 41.16; H, 4.74; N, 5.94. Found: C, 40.89; H, 4.50; N, 6.82. FT-IR (KBr, cm^{-1}): 3462 (s), 3591 (s), 3461 (br), 2971 (s), 2871 (w), 1650 (br), 1465 (m), 1333 (s), 1184 (s), 1079 (s), 981 (s), 883 (s), 801 (s), 694 (m), 541 (s). ^{1}H NMR (DMSO-d_6, 400 MHz): δ 7.60 (t, $^{3}J_{HH}$ = 7.1 Hz, 4H, pyr), 7.28 (br, 4H, pyr), 7.07 (s, 8H, Ar), 6.75 (d, $^{3}J_{HH}$ = 8.3 Hz, 4H, pyr), 6.50 (t, $^{3}J_{HH}$ = 6.2 Hz, 4H, pyr), 6.43(br, 8H, −NH_2), 3.69 (m, $^{3}J_{HH}$ = 6.8 Hz, 8H, ^{i}Pr−CH), 1.02 (d, $^{3}J_{HH}$ = 6.8 Hz, 48H, ^{i}Pr−CH_3) ppm. ^{31}P NMR (DMSO-d_6, 161 MHz): δ −5.9 ppm. TGA: temperature range (weight loss): 30−268 °C (∼2.5%); 268−340 °C (34.0%); 340−500 °C (∼29.5%); 500−830 °C (∼5.0%); 830−1030 °C (∼20.5%). ESI-MS: *m*/*z* calc. for [{Zn(Br-dipp)(2apy)}$_4$·2MeOH] 2042.5149; found 1978.9795 [M−2MeOH+H]$^+$.

6. Yield: 0.39 g (72%). Mp: >290 °C. Anal. Calcd for $C_{70}H_{96}N_8I_4O_{16}P_4Zn_4$ (M_r = 2166.6): C, 37.96; H, 4.34; N, 5.02. Found: C, 38.27; H, 4.12; N, 5.56. FT-IR (KBr, cm^{-1}): 3457 (m), 3357 (m), 3225 (w), 2962 (s), 2926 (s), 1638 (s), 1567 (m), 1498 (s), 1451 (s), 1337 (m), 1186 (s), 1022 (s), 911 (m), 773 (s), 606 (w), 544 (w). ^{1}H NMR (DMSO-d_6, 400 MHz) δ 7.50 (t, $^{3}J_{HH}$ = 7.1 Hz, 4H, pyr), 7.39 (br, 4H pyr) 7.25 (s, 8H, Ar), 6.58 (d, $^{3}J_{HH}$ = 8.2 Hz, 4H, pyr), 6.44 (t, $^{3}J_{HH}$ = 6.2 Hz, 4H, pyr), 6.36 (br, 8H, −NH_2), 3.53 (septet, 8H, $^{3}J_{HH}$ = 6.8 Hz, *i*Pr−CH), 0.98 (d, $^{3}J_{HH}$ = 6.8 Hz, 48H, ^{i}Pr−CH_3) ppm. ^{31}P NMR (DMSO-d_6, 161 MHz): δ −5.7 ppm. TGA: temperature range (weight loss): 30−270 °C (∼2.5%); 270−350 °C (∼33.5%); 350−500 °C (∼30.0%); 500−830 °C (∼5.0%); 830−1030 °C (∼20.5%). ESI-MS: *m*/*z* calc. for [{Zn(I-dipp)(2apy)}$_4$·2MeOH] 2166.8635; found 2166.8473 [M+H]$^+$.

5.4. Synthesis of Square-Wave Polymers 7−9. To a filtered solution of X-dippH_2 (X = Cl 0.073 g, Br 0.084 g, I 0.096 g, 0.25 mmol) and $[Zn(OAc)_2{\cdot}2H_2O]$ (0.055 g, 0.25 mmol) in methanol (30 mL) obtained after stirring, was added a solution of 4-CNpy (0.027 g, 0.25 mmol) in methanol. The resultant clear solution was kept for crystallization at room temperature to yield crystalline compounds **7**−**9** after 2 weeks.

7. Yield: 0.28 g (66.0%). Mp: >250 °C. Anal. Calcd for $C_{62}H_{84}N_4Cl_4O_{20}P_4Zn_4$ (M_r = 1696.6): C, 42.98; H, 4.89; N, 3.23. Found: C, 43.28; H, 4.30; N, 4.04. FT-IR (KBr, cm^{-1}): 3434 (br), 2966 (s), 2928 (m), 2869 (m), 1616 (s), 1466 (w), 1435 (m), 1337 (w), 1161 (s), 1020 (s), 922 (s), 887 (s), 830 (s), 560 (s). ^{1}H NMR (DMSO-d_6, 500 MHz) δ 8.38 (d, $^{3}J_{H-H}$ = 6.0 Hz, 4H, 4CNpy, Ar), 7.86 (d, $^{3}J_{H-H}$ = 6.0 Hz, 4H, 4CNpy, Ar), 7.02 (s, 8H, Cl-dipp, Ar), 4.13 (m, $^{3}J_{H-H}$ = 5.2 Hz, 2H, MeOH, −OH), 3.63 (septet, $^{3}J_{H-H}$ = 6.8 Hz, 8H, ^{i}Pr−CH), 3.16 (d, $^{3}J_{H-H}$ = 5.2 Hz, 2H, MeOH, −CH_3),

DOI: 10.1021/acs.inorgchem.5b00495
Inorg. Chem. 2015, 54, 4882−4894

Table 2. Crystal Data Details of Compounds 1−8 and 10−12

	1	2	3	4	5	6	7	8	10	11	12
CCDC[a] No.	1009221	1009222	1009223	1009224	1009225	1009226	1051180	1051181	1051182	1051183	1051184
empirical formula	$C_{80}H_{108}Cl_4N_4O_{16}P_4Zn_4$	$C_{80}H_{108}Br_4N_4O_{16}P_4Zn_4$	$C_{80}H_{108}I_4N_4O_{16}P_4Zn_4$	$C_{70}H_{96}Cl_4N_8O_{18}P_4Zn_4$	$C_{70}H_{96}Br_4N_8O_{18}P_4Zn_4$	$C_{70}H_{96}I_4N_8O_{18}P_4Zn_4$	$C_{31}H_{42}Cl_2N_2O_{10}P_2Zn_2$	$C_{31}H_{42}Br_2N_2O_{10}P_2Zn_2$	$C_{62}H_{88}Cl_4N_8O_{18}P_4Zn_4$	$C_{50}H_{64}Cl_2N_4O_{14}P_2Zn_2$	$C_9H_{13}O_5PZn$
formula wt, Fw	1908.86	2086.70	2274.66	1864.71	2042.55	2230.51	866.29	955.19	1760.64	1208.67	297.55
temp [K]	150(2)	150(2)	150(2)	293(2)	150(2)	150(2)	150(2)	150(2)	150(2)	150(2)	150(2)
crystal system	tetragonal	tetragonal	tetragonal	triclinic	orthorhom.	monoclinic	monoclinic	monoclinic	orthorhom.	triclinic	monoclinic
sace group	$\bar{I}4$	$\bar{I}4$	$\bar{I}4$	$\bar{P}1$	$P2_12_12$	$C2/c$	$P2_1/n$	$P2_1/n$	Fdd 2	$\bar{P}1$	$P2/c$
a [Å]	12.061(3)	12.102(4)	12.123(2)	10.1897(1)	21.4282(7)	31.442(8)	9.9660(4)	10.009(4)	30.291(4)	9.435(7)	14.445(6)
b [Å]	12.061(3)	12.102(4)	12.123(2)	15.5775(1)	20.1985(7)	10.244(2)	22.8187(1)	23.2864(1)	34.922(4)	11.301(9)	5.2832(2)
c [Å]	30.830(2)	31.228(1)	31.467(7)	29.698(4)	10.1981(3)	28.059(7)	17.5040(7)	17.488(8)	14.9814(2)	14.134(11)	15.690(6)
α [°]				78.052(7)						75.87(4)	
β [°]				80.542(7)		103.138(3)	98.620(1)	97.90(1)		76.14(4)	105.490(8)
γ [°]				66.159(6)						73.98(4)	
V [Å^3]	4484.0(8)	4574.0(3)	4624.6(1)	4200.4(1)	4413.9(2)	8801.0(2)	3935.6(4)	4037.3(4)	15848.0(3)	1380.5(2)	1153.9(8)
Z	2	2	2	2	2	4	4	4	8	1	4
D(calcd) [Mg/c-m^3]	1.414	1.515	1.634	1.474	1.537	1.683	1.462	1.572	1.476	1.454	1.713
μ [mm^{-1}]	1.310	2.915	2.490	1.400	3.022	2.618	1.488	3.298	1.479	1.090	2.269
θ range [°]	1.32−24.99	2.61−25.50	2.57−25.50	2.67- 25.00	3.42−25.00	2.65−24.99	2.68−25.50	2.65−25.00	2.93−25.50	2.60−25.50	1.98−25.00
reflns: collec./ indep.	16709/3953	17562/4248	17982/4308	31700/14596	34384/7751	32650/7754	24541/7932	27881/7093	30128/6322	10532/5071	11032/5271
goodness of fit, GOF	1.074	0.961	1.073	1.467	0.868	1.122	1.221	1.208	1.115	1.151	0.143
$R1(I_0 > 2\sigma(I_0))$	0.036	0.0569	0.040	0.099	0.033	0.055	0.080	0.090	0.025	0.095	0.055
$wR2$ (all data)	0.1147	0.1561	0.1156	0.3294	0.0714	0.1515	0.1350	0.1723	0.0727	0.2416	0.1098
largest hole and peak [e Å^{-3}]	0.615, −0.857	1.372, −1.832	1.111, −0.253	4.396, −1.259	0.775, −0.404	1.497, −1.780	0.740, −0.630	1.719, −1.087	0.570, −0.430	0.656, −0.926	0.854, −0.532

[a]CCDC = Cambridge Crystallographic Data Centre.

DOI: 10.1021/acs.inorgchem.5b00495
Inorg. Chem. 2015, 54, 4882−4894

1.09 (d, $^3J_{H-H}$ = 6.8 Hz, 48H, ^{i}Pr−CH$_3$) ppm. ^{31}P NMR (DMSO-d_6, 202 MHz): δ −5.4 ppm. TGA: temperature range (weight loss): 30−200 °C (∼9.0%); 200−400 °C (∼62.5%); 400−800 °C (∼5.0%); 800−1100 °C (∼16.0%).

8. Yield: 0.30 g (62.8%). Mp: >250 °C. Anal. Calcd for $C_{62}H_{84}N_4Br_4O_{20}P_4Zn_4$ (M_r = 1910.4): C, 38.26; H, 4.56; N, 2.88. Found: C, 38.25; H, 4.54; N, 2.49. FT-IR (KBr, cm^{-1}): 3426 (w), 2965 (s), 2926 (s), 2869 (m), 1617 (s), 1465 (m), 1336 (s), 1183 (s), 1116 (s), 1021 (s), 920 (s), 805 (s), 560 (w). ^{1}H NMR (DMSO-d_6, 500 MHz) δ 8.85 (d, $^3J_{H-H}$ = 6.0 Hz, 4H, 4CNpy, Ar), 7.87 (d, $^3J_{H-H}$ = 6.0 Hz, 4H, 4CNpy, Ar), 7.15 (s, 8H, Cl-dipp, Ar), 4.13 (m, $^3J_{H-H}$ = 5.2 Hz, 2H, MeOH, −OH), 3.63 (septet, $^3J_{H-H}$ = 6.8 Hz, 8H, ^{i}Pr−CH), 3.16 (d, $^3J_{H-H}$ = 5.2 Hz, 2H, MeOH, −CH$_3$), 1.09 (d, $^3J_{H-H}$ = 6.8 Hz, 48H, ^{i}Pr−CH$_3$) ppm. ^{31}P NMR (DMSO-d_6, 202 MHz): δ −5.5 ppm. TGA: temperature range (weight loss): 30−150 °C (∼7.0%); 150−400 °C (∼62.0%); 400−800 °C (∼7.5%); 800−1100 °C (∼12.5%).

9. Yield: 0.30 g (57.2%). Mp: >250 °C. Anal. Calcd for $C_{62}H_{84}N_4I_4O_{20}P_4Zn_4$ (M_r = 2098.5): C, 36.11; H, 3.91; N, 2.79. Found: C, 36.21; H, 3.91; N, 3.48. FT-IR (KBr, cm^{-1}): 2967 (s), 2867 (m), 1624 (s), 1574 (w), 1455 (m), 1388 (w), 1187 (s), 1020 (s), 909 (w), 822 (s), 688 (w), 543 (w). ^{1}H NMR (DMSO-d_6, 500 MHz) δ 8.83 (d, $^3J_{H-H}$ = 6.0 Hz, 4H, 4CNpy, Ar), 7.88 (d, $^3J_{H-H}$ = 6.0 Hz, 4H, 4CNpy, Ar), 7.20 (s, 8H, Cl-dipp, Ar), 4.13 (m, $^3J_{H-H}$ = 5.2 Hz, 2H, MeOH, −OH), 3.63 (septet, $^3J_{H-H}$ = 6.8 Hz, 8H, ^{i}Pr−CH), 3.16 (d, $^3J_{H-H}$ = 5.2 Hz, 2H, MeOH, −CH$_3$), 1.09 (d, $^3J_{H-H}$ = 6.8 Hz, 48H, ^{i}Pr−CH$_3$) ppm. ^{31}P NMR (DMSO-d_6, 202 MHz): δ −5.5 ppm. TGA: temperature range (weight loss): 30−200 °C (∼6.0%); 200−400 °C (∼66.5%); 400−800 °C (∼3.0%); 800−1100 °C (∼17.0%).

5.5. Synthesis of 10. To a solution of Cl-dippH$_2$ (0.073 g, 0.25 mmol) and [Zn(OAc)$_2$.2H$_2$O] (0.055 g, 0.25 mmol) in methanol (30 mL), was added a solution of imidazole (0.067 g, 1.00 mmol) in methanol. The resultant clear solution was filtered and kept for crystallization at room temperature to yield crystalline compounds **10** after 1 week. Yield: 0.35 g (89.7%). Mp: >250 °C. Anal. Calcd for $C_{62}H_{84}N_8Cl_4O_{18}P_4Zn_4$ (M_r = 1756.6): C, 42.39; H, 4.82; N, 6.38. Found: C, 42.78; H, 4.39; N, 5.20. FT-IR (KBr, cm^{-1}): 3669 (s), 3401 (s); 2963 (s), 2867 (m), 1583 (s), 1519 (s),1431 (s), 1336 (s), 1191 (w), 1152 (s), 1017 (s), 905 (s), 819 (s), 729 (s), 681 (s), 537 (s). ^{1}H NMR (DMSO-d_6, 500 MHz): δ 12.89 (br, 4H, Imz, N−H), 8.38 (s, 4H, Imz, Ar), 6.95(s, 8H, Cl-dipp, Ar), 6.94 (s, 8H, Imz, Ar), 3.65 (septet, $^3J_{H-H}$ = 6.8 Hz, 8H, ^{i}Pr−CH), 0.98 (d, $^3J_{H-H}$ = 6.8 Hz, 48H, ^{i}Pr−CH$_3$) ppm. ^{31}P NMR (DMSO-d_6, 202 MHz): δ −6.1 ppm. TGA: temperature range (weight loss): 30−225 °C (∼3.0%); 225−400 °C (∼60.0%); 400−800 °C (∼6.5%); 800−1100 °C (∼18.5%).

5.6. Synthesis of 11. To a solution of Cl-dippH$_2$ (0.073 g, 0.25 mmol) and [Zn(OAc)$_2$·2H$_2$O] (0.055 g, 0.25 mmol) in methanol (30 mL), was added a solution of 1,10-phenanthroline (0.054 g, 0.25 mmol) in methanol. The resultant clear solution was filtered and kept for crystallization at room temperature to yield crystalline compounds **11** after 1 week. Yield: 0.35 g (83.0%). Mp: >250 °C. Anal. Calcd for $C_{49}H_{56}N_4Cl_2O_{11}P_2Zn_2$ (M_r = 1140.6): C, 51.39; H, 4.95; N, 4.91. Found: C, 50.98; H, 4.50; N, 4.42. FT-IR (KBr, cm^{-1}): 3466 (br), 2966 (s), 2872 (s), 1622 (s), 1426 (s), 1332 (s), 1190 (s),1021 (s), 920 (s), 832 (s), 697 (m), 548 (s). ^{1}H NMR (DMSO-d_6, 500 MHz): δ 8.48 (d, 4H, phen), 8.38 (d, 4H, phen), 7.93 (s, 4H, phen), 7.58 (m, 4H, phen), 6.95 (s, 4H, Cl-dipp, Ar), 3.65 (septet, $^3J_{H-H}$ = 6.8 Hz, 8H, ^{i}Pr−CH), 0.98 (d, $^3J_{H-H}$ = 6.8 Hz, 48H, ^{i}Pr−CH$_3$) ppm. ^{31}P NMR (DMSO-d_6, 202 MHz): δ −5.9 ppm. TGA: temperature range (weight loss): 30−100 °C (∼10.0%); 100−400 °C (∼47.5%); 400−1000 °C (∼35.0%).

5.7. Synthesis of 12. A solution of [Zn(NO$_3$)$_2$·6H$_2$O] (0.148 g, 0.50 mmol) in methanol (15 mL) was added to a solution of dmppH$_2$ (0.101 g, 0.50 mmol) in methanol (15 mL) to yield colorless solution, which was filtered to yield crystalline compounds **12** after 3 days at room temperature. Yield: 0.08 g (57.0%). Mp: >250 °C. Anal. Calcd for $C_9H_{13}O_4PZn$ (M_r = 281.58): C, 38.39; H, 4.65. Found: C, 38.28; H, 4.52. FT-IR (KBr, cm^{-1}): 3367 (br), 3002 (s), 2925 (s), 2855 (m), 1635 (s), 1492 (s), 1437 (m), 1384 (s), 1151 (s), 1116 (s), 1030 (s), 929 (s), 848 (s), 519 (s). ^{1}H NMR (DMSO-d_6, 500 MHz): δ 7.02 (t, 1H, Ar), 6.80 (d, 2H, Ar), 2.10 (s, 6H, −CH$_3$) ppm. ^{31}P NMR (DMSO-d$_6$, 202 MHz): δ −4.32 ppm. TGA: temperature range (weight loss): 30−200 °C (∼3.5%); 200−400 °C (∼34.0%); 400−800 °C (∼5.0%); 800−1100 °C (∼13.5%).

5.8. Single-Crystal X-ray Diffraction Studies. Single crystals of compounds **1**−**8** and **10**−**12** were directly obtained from the reaction mixture via slow evaporation of the solvent at room temperature. Although attempted multiple times, crystals of **9** did not give good diffraction data. The crystals were mounted in paratone oil on a Rigaku Saturn 724+ ccd diffractometer for unit-cell determination and 3-D intensity data collection. Data integration and indexing was carried out using Crystalclear and structures were solved using direct method SIR-92.[21] The complete refinement calculations were carried using programs in WinGX module.[22] The final refinement of structures was carried out using full least-squares methods on F^2 using SHELXL-97.[23] Details of crystal data and structure refinement are given in Table 2.

■ ASSOCIATED CONTENT

Ⓢ Supporting Information

Synthesis, crystallographic details, additional figures, and spectral characterization. Crystallographic data of **1** (CCDC No. 1009221), **2** (CCDC No. 1009222), **3** (CCDC No. 1009223), **4** (CCDC No. 1009224), **5** (CCDC No. 1009225), **6** (CCDC No. 1009226), **7** (CCDC No. 1051180), **8** (CCDC No. 1051181), **10** (CCDC No. 1051183), **11** (CCDC No. 1051184), and **12** (CCDC No. 1051184). The Supporting Information is available free of charge on the ACS Publications website at DOI: 10.1021/acs.inorgchem.5b00495.

■ AUTHOR INFORMATION

Corresponding Author

*Tel.: +91 22 2576 7163. Fax: +91 22 2572 3480. E-mail: rmv@chem.iitb.ac.in.

Notes

The authors declare no competing financial interest.

■ ACKNOWLEDGMENTS

This work was supported by Nano Mission (DST), New Delhi; SERB (DST), New Delhi; and DAE (BRNS), Mumbai. R.M. thanks BRNS for the award of DAE-SRC Outstanding Investigator Award and DST for a J. C. Bose fellowship. A.A.D. and S.K.S. thank UGC for a research fellowship.

■ REFERENCES

(1) Wilson, S. T.; Lok, B. M.; Messina, C. A.; Cannan, T. R.; Flanigen, E. M. *J. Am. Chem. Soc.* **1982**, *104*, 1146.

(2) (a) Alvarez, C.; Llavona, R.; Garcia, J. R.; Suajrez, M.; Rodriguez, J. *Inorg. Chem.* **1987**, *26*, 1045. (b) Shah, B.; Chudasama, U. *Desalin. Water Treat.* **2012**, *38*, 227. (c) Hutchings, G. J. *J. Mater. Chem.* **2004**, *14*, 3385. (d) Muneyama, E.; Kunishige, A.; Ohdan, K.; Ai, M. *J. Catal.* **1996**, *158*, 378. (e) Wang, Y.; Wang, X. X.; Su, Z.; Guo, Q.; Tang, Q. H.; Zhang, Q. H.; Wan, H. L. *Catal. Today* **2004**, *93*, 155. (f) Lin, R. H.; Ding, Y. J.; Gong, L. F.; Dong, W. D.; Wang, J. H.; Zhang, T. *J. Catal.* **2010**, *272*, 65. (g) Kamiya, Y.; Nishikawa, E.; Satsuma, A.; Yoshimune, M.; Okuhara, T. *Microporous Mesoporous Mater.* **2002**, *54*, 277. (h) Alberti, G.; Casciola, M.; Marmottini, F.; Vivani, R. *J. Porous Mater.* **1999**, *6*, 299. (i) Kleitz, F.; Thomson, S. J.; Liu, Z.; Terasaki, O.; Schuth, F. *Chem. Mater.* **2002**, *14*, 4134. (j) Yuan, Z. Y.; Ren, T. Z.; Azioune, A.; Pireaux, J. J.; Su, B. L. *Catal. Today* **2005**, *105*, 647. (k) Yu, J.; Wang, A.; Tan, J.; Li, X.; van Bokhoven, J. A.; Hu, Y. K. *J. Mater. Chem.* **2008**, *18*, 3601. (l) Sarkar, A.; Pramanik, P. *Microporous Mesoporous Mater.* **2009**, *117*, 580.

(3) (a) Nonglaton, G.; Benitez, I. O.; Guisle, I.; Pipeler, M.; Leger, J.; Dubreuil, D.; Tellier, C.; Talham, D. R.; Bujoli, B. *J. Am. Chem. Soc.* **2004**, *126*, 1497. (b) Bhaumik, A.; Inagaki, S. *J. Am. Chem. Soc.* **2001**,

DOI: 10.1021/acs.inorgchem.5b00495
Inorg. Chem. 2015, 54, 4882−4894

123, 691. (c) Katz, H. E.; Scheller, G.; Putvinski, T. M.; Schilling, M. L.; Wilson, W. L.; Chidsey, C. E. D. *Science* **1991**, *6*, 1485. (d) Li, X. S.; Courtney, A. R.; Yantasee, W.; Mattigod, S. V.; Fryxell, G. E. *Inorg. Chem. Commun.* **2006**, *9*, 293. (e) Dutta, A.; Patra, A. K.; Bhaumik, A. *Microporous Mesoporous Mater.* **2012**, *155*, 208. (f) Kandori, K.; Nakashima, H.; Ishikawa, T. *J. Colloid Interface Sci.* **1993**, *160*, 499. (g) Padhi, A. K.; Nanjundaswamy, K. S.; Masquelier, C.; Okada, S.; Goodenough, J. B. *J. Electrochem. Soc.* **1997**, *144*, 1609. (h) Tian, X. Y.; He, W.; Cui, J. J.; Zhang, X. D.; Zhou, W. J.; Yan, S. P.; Sun, X. N.; Han, X. X.; Han, S. S.; Yue, Y. Z. *J. Colloid Interface Sci.* **2010**, *343*, 344.

(4) (a) Rodriguez-Liviano, S.; Aparicio, F. J.; Rojas, T. C.; Hungria, A. B.; Chinchilla, L. E.; Ocana, M. *Cryst. Growth Des.* **2012**, *12*, 635. (b) Luo, Q. L.; Shen, S. D.; Lu, G. Z.; Xiao, X. Z.; Mao, D. S.; Wang, Y. Q. *J. Mater. Chem.* **2009**, *19*, 8079. (c) Kononova, S. V.; Nesmeyanova, M. A. *Biochemistry (Moscow)* **2002**, *67*, 184. (d) Gielen, M.; Tiekink, E. R. T. *Metallotherapeutic Drugs and Metal-Based Diagnostic Agents: The Use Of Metals In Medicine*; John Wiley & Sons, Ltd.: Hoboken, NJ, 2005. (e) Kim, T. W.; Chung, P. W.; Slowing, I. I.; Tsunoda, M.; Yeung, E. S.; Lin, V. S. Y. *Nano Lett.* **2008**, *8*, 3724. (f) Liu, J. W.; Stace-Naughton, A.; Jiang, X. M.; Brinker, C. J. *J. Am. Chem. Soc.* **2009**, *131*, 1354.

(5) (a) Nishiyama, Y.; Tanaka, S.; Hillhouse, H. W.; Nishiyama, N.; Egashira, Y.; Ueyama, K. *Langmuir* **2006**, *22*, 9469. (b) Tian, B. Z.; Liu, X. Y.; Tu, B.; Yu, C. Z.; Fan, J.; Wang, L. M.; Xie, S. H.; Stucky, G. D.; Zhao, D. Y. *Nat. Mater.* **2003**, *2*, 159. (c) Sahu, A. K.; Pitchumani, S.; Sridhar, P.; Shukla, A. K. *Fuel Cells* **2009**, *9*, 139. (d) Jimenez-Jimenez, J.; Maireles-Torres, P.; Olivera-Pastor, P.; Rodriguez-Castellon, E.; Jimenez-Lopez, A.; Jones, D. J.; Roziere, J. *Adv. Mater.* **1998**, *10*, 812. (e) Rodriguez-Castellon, E.; Jimenez-Jimenez, J.; Jimenez-Lopez, A.; Maireles-Torres, P.; Ramos-Barrado, J. R.; Jones, D. J.; Roziere, J. *Solid State Ionics* **1999**, *125*, 407.

(6) Kalita, A. C.; Gogoi, N.; Jangir, R.; Kuppuswamy, S.; Walawalkar, M. G.; Murugavel, R. *Inorg. Chem.* **2014**, *53*, 8959.

(7) (a) Cheetham, A. K.; Férey, G.; Loiseau, T. *Angew. Chem., Int. Ed.* **1999**, *38*, 3268. (b) Rao, C. N. R.; Natarajan, S.; Choudhury, A.; Neeraj, S.; Ayi, A. A. *Acc. Chem. Res.* **2001**, *34*, 80. (c) Finn, R. C.; Zubieta, J.; Haushalter, R. C. *Prog. Inorg. Chem.* **2003**, *51*, 421−601. (d) Clearfield, A. *Prog. Inorg. Chem.* **1998**, *47*, 371. (e) Cao, G.; Hong, H.-G.; Mallouk, T. E. *Acc. Chem. Res.* **1992**, *25*, 420.

(8) (a) Katovic, A.; Giordano, G.; Kowalak, S. *Stud. Surf. Sci. Catal. A* **2002**, *142*, 39. (b) Tischendorf, B. C.; Alam, T. M.; Cygan, R. T.; Otaigbe, J. U. *J. Non-Cryst. Solids* **2003**, *316*, 261. (c) Simon-Masseron, A.; Paillaud, J. L.; Patarin, J. *Chem. Mater.* **2003**, *15*, 1000. (d) Lin, Z. E.; Yao, Y. W.; Zhang, J.; Yang, G. Y. *J. Chem. Soc., Dalton Trans.* **2002**, 4527. (e) Chen, X. M.; Zhao, Y. N.; Wang, R. J.; Ming, L. A.; Mai, Z. H. *J. Chem. Soc., Dalton Trans.* **2002**, 3092. (f) Liu, Y. L.; Liu, W.; Xing, Y.; Shi, Z.; Fu, Y. L.; Pang, W. Q. *J. Solid State Chem.* **2002**, *166*, 265. (g) Jensen, T. R.; Hazell, R. G.; Christensen, A. N.; Hanson, J. C. *J. Solid State Chem.* **2002**, *166*, 341. (h) Zhao, Y. N.; Ju, J.; Chen, X. M.; Li, X. H.; Wang, Y.; Wang, R. J.; Li, M.; Mai, Z. H. *J. Solid State Chem.* **2002**, *166*, 369. (i) Zhao, Y. N.; Yao, Y. W.; Li, X. H.; Chen, X. M.; Li, M.; Mai, Z. H. *Chem. Lett.* **2002**, 542. (j) Natarajan, S. *J. Chem. Soc., Dalton Trans.* **2002**, 2088.

(9) (a) Bu, X.; Feng, P.; Gier, T. E.; Stucky, G. D. *J. Solid State Chem.* **1998**, *136*, 210. (b) Feng, P.; Bu, X.; Stucky, G. D. *Angew. Chem., Int. Ed. Engl.* **1995**, *34*, 1745. (c) Gier, T. E.; Stucky, G. D. *Nature* **1991**, *349*, 508. (d) Nenoff, T. M.; Harrison, W. T. A.; Gier, T. E.; Stucky, G. D. *J. Am. Chem. Soc.* **1991**, *113*, 378. (e) Harrison, W. T. A.; Gier, T. E.; Moran, K. L.; Nicol, J. M.; Eckert, H.; Stucky, G. D. *Chem. Mater.* **1991**, *3*, 27. (f) Song, T.; Xu, J.; Zhao, Y.; Yue, Y.; Xu, Y.; Xu, R.; Hu, N.; Wei, G.; Jia, H. *J. Chem. Soc. Chem. Commun.* **1994**, 1171. (g) Murugavel, R.; Walawalker, M. G.; Pothiraja, R.; Rao, C. N. R.; Choudhury, A. *Chem. Rev.* **2008**, *108*, 3549.

(10) (a) Lugmair, C. G.; Tilley, T. D.; Rheingold, A. L. *Chem. Mater.* **1997**, *9*, 339. (b) Yang, Y.; Pinkas, J.; Noltemeyer, M.; Roesky, H. W. *Inorg. Chem.* **1998**, *37*, 6404. (c) Anantharaman, G.; Chandrasekhar, V.; Walawalkar, M. G.; Roesky, H. W.; Vidovic, D.; Magull, J.; Noltemeyer, M. *J. Chem. Soc., Dalton Trans.* **2004**, 1271. (d) Yang, Y.; Pinkas, J.; Roesky, H. W.; Schäfer, M. *Angew. Chem., Int. Ed.* **1998**, *37*, 2650.

(11) (a) Neeraj, S.; Natarajan, S.; Rao, C. N. R. *Angew. Chem., Int. Ed.* **1999**, *38*, 3480. (b) Francis, R. J.; O'Brien, S.; Fogg, A. M.; Halasyamani, P. S.; O'Hare, D.; Loiseau, T.; Férey, G. *J. Am. Chem. Soc.* **1999**, *121*, 1002. (c) Haouas, M.; Gerardin, C.; Taulelle, F.; Estournes, C.; Loiseau, T.; Férey, G. *Colloids Interfaces A* **1999**, *158*, 229. (d) Férey, G. *Chem. Mater.* **2001**, *13*, 3084. (e) Férey, G. *J. Fluorine Chem.* **1995**, *72*, 187. (f) Férey, G. *C. R. Acad. Sci. Ser. II* **1998**, *1*, 1. (g) Rao, C. N. R.; Natarajan, S.; Choudhury, A.; Neeraj, S.; Vaidhyanathan, R. *Acta Crystallogr.* **2001**, *B57*, 1.

(12) (a) Cheetham, A. K.; Ferey, G.; Loiseau, T. *Angew. Chem., Int. Ed.* **1999**, *38*, 3268. (b) Oliver, S.; Kuperman, A.; Ozin, G. A. *Angew. Chem., Int. Ed.* **1998**, *37*, 47.

(13) (a) Chidambaram, D.; Neeraj, S.; Natarajan, S.; Rao, C. N. R. *J. Solid State Chem.* **1999**, *147*, 154. (b) Ayyappan, S.; Bu, X.; Cheetham, A. K.; Natarajan, S.; Rao, C. N. R. *Chem. Commun.* **1998**, 218.

(14) (a) Neeraj, S.; Natarajan, S.; Rao, C. N. R. *J. Solid State Chem.* **2000**, *150*, 417. (b) Natarajan, S.; van Wullen, L.; Klein, W.; Jansen, M. *Inorg. Chem.* **2003**, *42*, 6265. (c) Harrison, W. T. A.; Hannooman, L. *J. Solid State Chem.* **1997**, *131*, 363. (d) Ayi, A. A.; Choudhury, A.; Natarajan, S.; Neeraj, S.; Rao, C. N. R. *J. Mater. Chem.* **2001**, *11*, 1181. (e) Ayyappan, S.; Cheetham, A. K.; Natarajan, S.; Rao, C. N. R. *J. Solid State Chem.* **1998**, *139*, 207. (f) Lin, Z.-E.; Yao, Y.-W.; Zhang, J.; Yang, G.-Y. *Dalton Trans.* **2003**, 3160.

(15) (a) Murugavel, R.; Kuppuswamy, S.; Boomishankar, R.; Steiner, A. *Angew. Chem., Int. Ed.* **2006**, *45*, 5536. (b) Murugavel, R.; Kuppuswamy, S.; Gogoi, N.; Boomishankar, R.; Steiner, A. *Chem.—Eur. J.* **2010**, *16*, 994.

(16) Dar, A. A.; Mallick, A.; Murugavel, R. *New J. Chem.* **2015**, *39*, 1186.

(17) (a) Murugavel, R.; Kuppuswamy, S.; Gogoi, N.; Steiner, A. *Inorg. Chem.* **2010**, *49*, 2153. (b) Murugavel, R.; Kuppuswamy, S.; Gogoi, N.; Steiner, A.; Boomishankar, R.; Suresh, K. G. *Chem.—Asian J.* **2009**, *4*, 143. (c) Kalita, A. C.; Roch-Marchal, C.; Murugavel, R. *Dalton Trans.* **2013**, *26*, 9755. (d) Gupta, S. K.; Kuppuswamy, S.; Walsh, J. P. S.; Mclnnes, E. J. L.; Murugavel, R. *Dalton Trans.* **2015**, *44*, 5587. (e) Gupta, S. K.; Dar, A. A.; Rajeshkumar, T.; Kuppuswamy, S.; Langley, S. K.; Murray, K. S.; Rajaraman, G.; Murugavel, R. *Dalton Trans.* **2015**, *44*, 5961. (f) Kalita, A. C.; Murugavel, R. *Inorg. Chem.* **2014**, *53*, 3345.

(18) Coxall, R. A.; Harris, S. G.; Henderson, D. K.; Parsons, S.; Tasker, P. A.; Winpenny, R. E. P. *J. Chem. Soc., Dalton Trans.* **2000**, 2349.

(19) Gamoke, B.; Neff, D.; Simons, J. *J. Phys. Chem. A* **2009**, *113*, 5677.

(20) *Vogel's Text Book of Practical Organic Chemistry*, 5th Edition; Langman Group: Essex, Harlow, U.K., 1989.

(21) Altomare, A.; Cascarano, G.; Giacovazzo, C.; Guagliardi, A.; Burla, M. C.; Polidori, G.; Camalli, M. *J. Appl. Crystallogr.* **1994**, *27*, 435.

(22) Farraugia, L. J. *J. Appl. Crystallogr.* **1999**, *32*, 837.

(23) Sheldrick, G. M. *Acta Crystallogr., Sect. A: Found. Crystallogr.* **2008**, *A64*, 112.

DOI: 10.1021/acs.inorgchem.5b00495
Inorg. Chem. 2015, 54, 4882−4894